Rational design of organic electro-optic materials

2003 J. Phys.: Condens. Matter 15 R897

(http://iopscience.iop.org/0953-8984/15/20/203)

INSTITUTE OF PHYSICS PUBLISHING JOURNAL OF PHYSICS: CONDENSED MATTER

J. Phys.: Condens. Matter **15** (2003) R897–R934 PII: S0953-8984(03)31017-3

TOPICAL REVIEW

Rational design of organic electro-optic materials

L R Dalton

Departments of Chemistry and Electrical Engineering, University of Washington, Seattle, WA 98195-1700, USA

E-mail: dalton@chem.washington.edu

Received 14 February 2003
Published 12 May 2003
Online at stacks.iop.org/JPhysCM/15/R897

Abstract

Quantum mechanical calculations are used to optimize the molecular first hyperpolarizability of organic chromophores and statistical mechanical calculations are used to optimize the translation of molecular hyperpolarizability to macroscopic electro-optic activity (to values of greater than 100 pm V^{-1} at telecommunications wavelengths). Macroscopic material architectures are implemented exploiting new concepts in nanoscale architectural engineering. Multi-chromophore-containing dendrimers and dendronized polymers not only permit optimization of electro-optic activity but also of auxiliary properties including optical loss (both absorption and scattering), thermal and photochemical stability and processability. New reactive ion etching and photolithographic techniques permit the fabrication of three-dimensional optical circuitry and the integration of that circuitry with semiconductor very-large-scale integration electronics and silica fibre optics. Electro-optic devices have been fabricated exploiting stripline, cascaded prism and microresonator device structures. Sub-1 V drive voltages and operational bandwidths of greater than 100 GHz have been demonstrated. Both single- and double-ring microresonators have been fabricated for applications such as active wavelength division multiplexing. Free spectral range values of 1 THz and per channel modulation bandwidths of 15 GHz have been realized permitting single-chip data rates of 500 Gb s^{-1}. Other demonstrated devices include phased array radar, optical gyroscopes, acoustic spectrum analysers, ultrafast analog/digital converters and ultrahigh bandwidth signal generators.

(Some figures in this article are in colour only in the electronic version)

Contents

1. Introduction

Electro-optic materials permit low (dc-50 THz) and high (optical) frequency electromagnetic fields to interact through the perturbation that their electrical components have on weakly bound electron distributions. For example, a radiofrequency field propagates through an electro-optic material producing significant perturbation of the electron distribution of the material. An optical field co-propagating through the same material is influenced by this perturbed distribution, e.g. the speed of light is reduced. Thus, an electro-optic material is said to provide voltage control of the index of refraction. A weakly bound electron distribution is usually synonymous with quasi-delocalization. The pi electronic structure of polyene and quasi-aromatic (and heteroaromatic) organic molecules fit this description. There are also symmetry requirements for molecular and macroscopic electro-optic activity (or, more generally, second-order optical nonlinearity). Either dipolar (noncentrosymmetric) or octupolar symmetry must exist at the molecular and macroscopic levels. To keep this review to a finite length, we restrict the discussion to dipolar chromophores and ferroelectric material lattices. The reader is referred elsewhere for an introduction to octupolar electro-optic materials [1, 2]. We shall shortly see that organic molecules can exhibit enormous molecular hyperpolarizability but that the translation of that molecular optical nonlinearity to macroscopic electro-optic activity is extremely difficult. The charge distribution of materials, and hence index of refraction, can also be changed by molecular reorientation of ordered molecular lattices under the influence of an applied electric field, e.g. liquid crystalline materials. Obviously, such effects can be very large: however, since response (switching) time will be defined by the mass moved, such effects will be much slower (millisecond to microsecond) than the purely 'electronic' electro-optic effects discussed here. Electro-optic materials are typically utilized for optical wavelength operation away from electronic transitions (resonances); thus the ultimate response time is the phase relaxation time of the pi-electron system. This time is typically of the order of tens to hundreds of femtoseconds so that operation into the terahertz (THz), as well as gigahertz (GHz), frequency domain is possible [3–7]. In reality, problems of delivering the low frequency (GHz or THz) signals to the material will limit practical device bandwidths [8, 9]. Nevertheless, devices based on organic electro-optic materials can commonly exhibit 3 dB bandwidths above 100 GHz and operation into the THz regime [3–5]. Clearly, a distinct advantage of organic electro-optic materials relative to liquid crystalline, inorganic electro-optic, inorganic electro-absorptive and inorganic modulated laser materials is their exceptional bandwidth potential. Both the index of refraction and dielectric permittivity are determined by the pi-electrons and both properties are relatively independent of frequency. This means that optical and long wavelength (radiowave, microwave and millimetre wave) fields propagate at the same velocity, permitting long interaction lengths to be exploited. Such is not the case with materials such as lithium niobate where very large dielectric constants (e.g. 32) lead to significant velocity

Table 1. Comparison of electro-optic materials and device parameters[a].

Parameter	$LiNbO_3$	NLO polymer
r_{eff} (pm V^{-1})	30	130
n^3 (r_{eff})[b]	330	584
Dielectric constant (ε)	30	3–4
Index of refraction (n)	2.2	1.6–1.7
n^3 $(r_{eff})/\varepsilon$[b]	10	195
Length–bandwidth product (GHz cm)	7	>100
$V_\pi L$ (V cm)	5	1–2
Optical loss (dB cm^{-1})	0.2	0.2–1.0
Crystal growth temperature (°C)	1000	NA
Waveguide processing temperature (°C)	1000	<300
Multiple layers possible	No	Yes
Fabrication and processing	Difficult	Simpler
Packaging	Expensive	Unknown

[a] At optical wavelength of 1.3 μm.
[b] Values given are figures of merit.

mismatch between optical and low frequency fields with consequences for bandwidth and/or drive voltage limitations. The high dielectric constants of inorganic materials such as lithium niobate lead to power dissipation, providing yet another advantage for the low dielectric constant (e.g. 3–4) organic materials. Table 1 compares the dielectric, index of refraction, electro-optic and optical loss properties of organic and lithium niobate electro-optic materials and some of the consequences of those parameter values for device characteristics.

While the potential for exceptional device bandwidths is one of the strong motivations for considering organic electro-optic materials, many other material properties must be simultaneously realized if organic electro-optic materials are to achieve commercial viability. These include sufficiently large electro-optic activity to permit reasonable drive voltage levels to be utilized with diverse device structures. Typically, drive voltages of 1 V or less will be required for many applications. This applies to both analog and digital data handling operations. For analog data, lossless transduction between the electrical and optical signal domains is desired. Gain or loss in the transduction process is defined by drive voltage requirement and hence electro-optic activity. A V_{pi} (the voltage required to produce a pi phase shift in the optical wave) of approximately 1 V is required for lossless transduction; smaller values lead to amplification (gain) of the electrical signal at the end of the electrical-to-optical-to-electrical signal transduction process. Dynamic range is also related to the drive voltage requirement. Both gain and dynamic range are quadratically related to electro-optic activity. For digital data, low drive voltages are required to avoid expensive digital amplifiers that also introduce bandwidth limitations. For satellite (space) based applications, weight is an additional important consideration and amplifiers necessary to step voltage levels up to that required for electro-optic modulator operation contribute to weight.

Total electro-optic device insertion loss must be of the order of 5 dB or less. There are two components to such loss, namely silica optical fibre to electro-optic waveguide coupling loss and electro-optic waveguide loss. Coupling loss must be kept to 1 dB or less per connection. Electro-optic waveguide loss (often referred to as material loss) is comprised of both absorption and scattering loss and must be, typically, of the order of 1 dB cm^{-1} or less. Obviously, material loss can limit electrical/optical interaction (device electrode) length to a few centimetres. Drive voltage, V_{pi}, will, of course, depend on interaction (device electrode) length. Thus, we see that bandwidth, drive voltage and optical loss issues are not independent.

Stability (thermal and photochemical) is important. In general, devices are expected to last approximately ten years, which commonly translates into minimum thermal stability (TS) requirements of no significant change in performance for one thousand hours at 85 °C and waveguide powers of the order of 20 mW. Of course, material stability requirements will vary both with specific application and device type. With organic electro-optic materials, TS does not refer to the temperature at which the material decomposes but rather the temperature at which noncentrosymmetric chromophore order is lost because of thermally induced motion of the lattice. For polymeric materials, this is related to the glass transition temperature of the electro-optic material. Non-bonding steric interactions, segmental flexibility of supramolecular structures and restrictions on motion associated with covalent bond potentials define TS. The concept of 'lattice hardness' is routinely invoked when speaking of TS—the more resistant the lattice to chromophore movement, the greater the TS of electro-optic activity. A convenient way to assess TS in a dynamic manner is to ramp the temperature of the material sample at 5–10 °C min^{-1} while monitoring macroscopic second-order optical nonlinearity (e.g. second harmonic generation [10], which is related to electro-optic activity). The TS is defined as the point at which optical nonlinearity is first observed to decrease in such an experiment. Typically, 'dynamic thermal stability' of the order of 150 °C is required to achieve long term (>1000 h) temporal stability at 85 °C. Fortunately, dynamic TS of 200 °C (or even greater) has been achieved by appropriate supramolecular engineering for side-chain polymer materials, three-dimensional crosslinked polymer materials and dendrimer (and dendronized polymer) materials.

Photochemical stability is dominated by singlet oxygen chemistry for organic materials. Stability is observed to depend on oxygen concentration, lattice hardness (oxygen diffusion rates), chromophore structures (sites sensitive to singlet oxygen attack) and upon the presence of singlet oxygen quenchers (scavengers). Interband absorption by electro-optic chromophores is important for the production of singlet oxygen. Thus it is important to shield electro-optic materials from visible wavelength light. Simple packaging, that minimizes oxygen concentration and exposure to visible wavelength light, appears to address the problem of photostability sufficiently to permit commercial application; however, this matter needs continued study and careful definition for each electro-optic material.

Of course, materials must be capable of being fabricated into devices and integrated with very-large-scale integration (VLSI) semiconductor electronics and silica fibre optics. Fortunately, polymeric and macromolecular organic electro-optic materials are exceptionally amenable to a variety of materials processing techniques including spin casting and electric field poling by both corona and electrode methods [11–15], sequential (layer by layer) synthesis by both Langmuir–Blodgett and Merrifield self-assembly methods [16–18] and reactive ion etching and photolithographic methods [19–36]. Direct and effective integration with VLSI semiconductor electronics and silica fibre optics has been demonstrated [19, 26]. The processability of organic electro-optic materials has facilitated the fabrication of stripline, cascaded prism, in-line fibre, microresonator and photonic bandgap device structures [19–41]. Moreover, circuitry and devices have been implemented in three-dimensional motifs [11, 28]. As already noted, drive voltages of the order of 1 V or less have been demonstrated [42–44] as well as 3 dB device bandwidths of 200 GHz [3]. Prototype devices ranging from acoustic spectrum analysers [45], to phased array radar [11, 46], to voltage-controlled add/drop wavelength filters [36, 37], to active wavelength division multiplexing (WDM) systems [36, 37], to analog-to-digital converters [47, 48], to spatial light modulators [38–40] have been demonstrated. In this review, we will discuss the fabrication of stripline, prism and microresonator devices and some of the applications of these classes of devices.

In the following sections, we review both the current status of, and future prognosis for, molecular hyperpolarizability and electro-optic activity development. Emphasis is placed on the theoretical methods that have guided molecular and macroscopic material improvements. The importance of auxiliary material properties such as optical loss, TS and photostability is discussed, as is the control of these properties by rational design. We then review the processing of electro-optic materials to fabricate active device structures and the evaluation of the performance of prototype devices. This review is largely restricted to the period from 1997 to the present. For review of earlier work, the reader is referred to previously published reviews and texts [11–15, 18, 26, 49–63].

2. Molecular hyperpolarizability

2.1. Theory

The active component of device quality organic electro-optic materials is a dipolar chromophore consisting of an electron donor moiety, a pi-electron bridge and an electron acceptor moiety (examples are provided in table 2 [26, 50, 64–71]). The parameter that describes the change in electron distribution of such chromophores in an applied electric field is the molecular first hyperpolarizability, β. Molecular hyperpolarizability is typically measured by methods such as electric-field-induced second harmonic generation (EFISH) and hyper-Rayleigh scattering (HRS). As these measurement techniques have been discussed elsewhere [11, 18, 26] they will not be reviewed here. In the case of dipolar chromophores, such as shown in table 2, β will be determined by the strength of the electron donor, the strength of the electron acceptor and the connectivity of the pi-electron bridge (which is usually discussed in terms of bond length alternation and the dihedral angles that define the relative spatial alignment of pi orbitals). Of course, these three features are inter-related and understanding molecular hyperpolarizability requires resorting to molecular quantum mechanics. Quantum mechanical calculations of atomic and molecular hyperpolarizability have been the subject of active investigation for several decades [72–113]. In the 1990s, Marder and co-workers [86–91] attempted to provide guidance to synthetic organic chemists attempting to prepare improved chromophores by discussing the relationship of molecular hyperpolarizability to molecular structural features. Their starting point was the simple two-state model of a charge transfer complex. In particular, for simple polyene and heteroaromatic bridge structures, they showed that molecular hyperpolarizability varied in a sinusoidal manner with bond length alternation. Because of this sinusoidal dependence and because of the dependence of bond length alternation on donor or acceptor strength, they showed that increasing donor and acceptor strength did not always lead to improved molecular hyperpolarizability. They demonstrated that, for a given donor and acceptor, molecular hyperpolarizability could be tuned by choosing bridge components (phenyl rings, thiophene rings, etc) with different aromaticities (hence different bond length alternation). Such structure/function guidance, expressed in terms familiar to the organic chemist, clearly has been helpful in advancing the performance of organic chromophores shown in table 2. In like manner, Garito and co-workers [114] demonstrated that exceptional hyperpolarizability could be achieved for fused ring chromophores. Unfortunately, large molecular hyperpolarizability is a necessary but not sufficient condition for a chromophore that can be translated into a useable electro-optic material. Several auxiliary conditions must apply, including the ability to synthesize the chromophore in reasonable yield and purity, the chromophore must be processable to the extent required for realizing a macroscopic noncentrosymmetric chromophore lattice by techniques such as electric field poling or sequential synthesis and the chromophore must

Table 2. $\mu\beta$ values for representative organic electro-optic chromophores.[a]

Chromophore base	R	Nonlinearity, μβ, esu × 10^{-48}
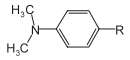		140[b,c]
	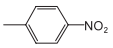	275[d]
	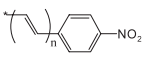	580[c], 482[f] (n=1) 813[f] (n=2) 1074[f] (n=3) 1700[f] (n=4)
	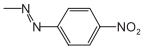	800[g,h] DR
	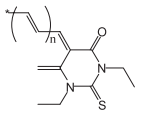	370[f] (n=0) 1457[f] (n=1) 3945[f] (n=2) 9831 (n=3)
	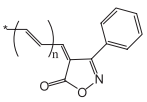	312[f] (n=0) 1202[f] (n=1) 3156[f] (n=2) 8171[f] (n=3)
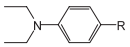	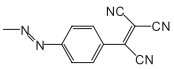	4100[g,h]
		560[d] (X=O, R'=NO_2) 700[d] (X=S, R'=NO_2)
		2400[i] (X=S, R'= )
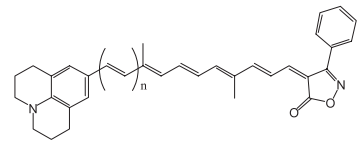		28,500[f]
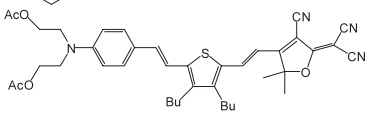		18,000[j] FTC
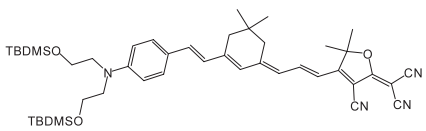		>30,000[k] CLD

[a] Measured at 1.907 μm unless otherwise indicated. μ is the dipole moment and β is the molecular first hyperpolarizability.
[b] Measured at 1.3 μm.
[c] Reference [65].
[d] Reference [66].
[e] Reference [67].
[f] Reference [69].
[g] Measured at 1.58 μm.
[h] Reference [68].
[i] Reference [70].
[j] Reference [26].
[k] Reference [71].

exhibit adequate thermal, chemical and photochemical stability. Thus, while fused ring chromophores exhibit exceptional molecular hyperpolarizability, their poor solubility in spin casting solvents and poor mobility under electric field poling conditions frequently renders them unusable. Unprotected polyene structures and certain donor and acceptor moieties do not exhibit adequate stability or prove impossible to prepare in high yield and purity.

Nevertheless, quantum mechanical guidance has promoted rapid improvement in chromophore molecular hyperpolarizability, as can be seen from table 2, which illustrates the evolution of molecular hyperpolarizability from 1990 to 2000. Some of the guidance is obvious; for example, molecular hyperpolarizability can be improved by making chromophores longer. However, there are limits to this paradigm due to the fact that ultimately steric effects and molecular motion act to limit the long range coupling of pi orbitals. This is analogous to the concept of persistence length for base pair interactions in polynucleotides. Moreover, chemical stability can be influenced by length as well as by electron donor and acceptor strength. There is obviously a balance that must be achieved in optimizing molecular hyperpolarizability (where the electronic structure returns to its original state after the electric field perturbation is removed) and chemical reactivity that occurs when charges separate and migrate to other molecules. Indeed, an important advance that occurred in the late 1990s was the introduction of the cyanofuran acceptor (see FTC and CLD chromophores of table 2). This acceptor permitted chromophores to be synthesized that were quite soluble in spin casting solvents and processable, exhibited thermal stability by thermogravimetric (TGA) and differential scanning calorimetry (DSC) to 300 °C and permitted molecular hyperpolarizability values of greater than[1] $15\,000 \times 10^{-48}$ esu to be routinely obtained. These chromophores have attracted considerable industrial attention; for example, Lockheed Martin [44] and Corning [115, 116] have explored systematic minor modification of these chromophores to improve properties. Corning has prepared variants of CLD that exhibit electro-optic coefficients of 75 pm V^{-1} at 1.55 μm telecommunications wavelength [116]. This latter number likely represents a record performance for the CLD chromophores incorporated into simple polymer systems. Both Lockheed Martin and TACAN Corporation (now IPITEK) achieved Mach–Zehnder modulators operating with V_{pi} drive voltage requirements of approximately 1 V using FTC (or CLD)/polymer composite materials [42–44]. Researchers at Lockheed Martin also made the important observation that replacing even a single methyl group on the cyanofuran moiety with a trifluoromethyl (CF_3) group (see figure 1) resulted in a significant improvement in molecular hyperpolarizability. This improvement, which is at first non-obvious, can be understood in terms of hyperconjugation. Other structural modifications (see figure 1) also resulted in large (e.g. factor of two) improvements in molecular hyperpolarizability. Recently, these have been reproduced by quantum mechanical calculations. An example is the case of selective replacement of cyano (CN) groups of the cyano furan moiety with nitro (NO_2) groups. Replacement of one or two cyano groups with nitro groups leads to increased hyperpolarizability compared to the tricyano acceptor. One cyano and two nitro groups are optimum and yield a value for hyperpolarizability larger than obtained for trinitrofuran. For example, consider the related prototype structures shown in figure 2 and the computational results shown in table 3 [117]. Note that, although substitution of ligands on the cyanofuran group can cause changes in the dihedral angle, the changes in dihedral angle cannot account for the changes in molecular hyperpolarizability associated with mixed ligand substitution. Changes in molecular conformation can be influenced by both electronic and steric (nuclear or packing) effects. A similar effect on molecular

[1] Unfortunately, the use of both electrostatic (esu) and SI units are common in electro-optics. Note that 1 (cm^5 esu^{-1} or esu) $= 4.19 \times 10^{-10}$ m^4 V^{-1}. Another useful conversion factor is 1 D (10^{-18} esu cm^{-1}) $= 3.336 \times 10^{-30}$ C m^{-1}.

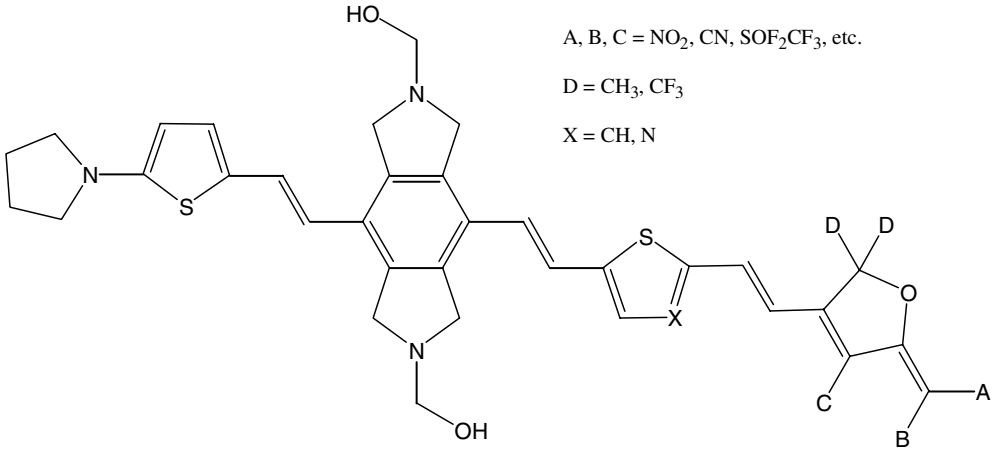

Figure 1. Various simple modifications of a generic chromophore structure are shown.

Table 3. Calculated β values and dihedral angles for various mixed ligand acceptor chromophores.

Chromophores	$\langle\beta\rangle$ (10^{-30} esu)	Dihedral angle
A	183	178
B	196	142
C	222	138
D	308	179
E	229	129
F	306	150
G	**357**	**178**
H	320	137
I	191	179
J	245	158
K	346	179
L	362	178
M	349	148
N	340	161
O	**415**	**176**
P	388	147

hyperpolarizability occurs when the heteroaromatic moiety nearest to the acceptor (see figure 1) is a thiazole (X = N) rather than thiophene (X = CH). This has been observed in theoretical calculations [98]. Relatively simple modification of the FTC and CLD chromophores of table 2 have led to hyperpolarizability values of $60\,000 \times 10^{-48}$ esu or greater. Recent results suggest that similar improvement in molecular hyperpolarizability can be achieved by modification of donor moieties. For example, azaphosphanes appear promising [118]. Although the rate of improvement of molecular hyperpolarizability in the future is very unlikely to equal that of the 1990s, some significant improvement can be expected. Current chromophores permit realization of materials exhibiting electro-optic coefficients at telecommunications wavelengths in the range 100–130 pm V^{-1}. The realization of electro-optic coefficients of greater than 300 pm V^{-1} is likely with expected improvements in molecular hyperpolarizability.

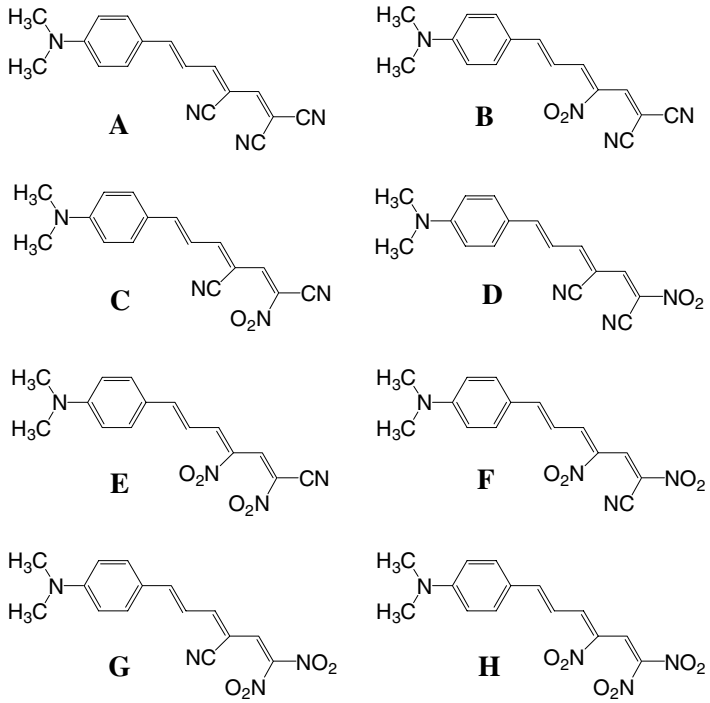

Figure 2. The chemical structures associated with the quantum mechanical results of table 3 are shown.

2.2. Chromophore synthesis

As already noted, realization of exceptional molecular hyperpolarizability is of little value if the chromophores cannot be synthesized in reasonable yield and purity and do not exhibit appropriate auxiliary properties. Of course, it is a misconception to think that organic electro-optic chromophores must be produced in ton quantities. Less than 50 mg of chromophores are required to spin coat a 6 inch wafer and many hundreds of modulators can be fabricated in such a thin film structure. As is frequently the case in high technology electronics and photonics, materials costs seldom compete with processing and packaging costs. Nevertheless, synthetic efficiency must be such to permit kilogram quantities of electro-optic materials to be prepared in finite time and at finite cost.

The synthesis shown in figure 3 illustrates the approximate level of complexity that can be tolerated. While multiple fused-ring thiophene [119] moieties lead to very good molecular hyperpolarizability, the synthetic difficulty of preparing chromophores with these units makes commercial utilization unlikely. Of course, synthetic routes to specific chromophores are constantly being improved [120–151]. A number of improvements have been made in the preparation of key intermediates [136–138]. However, one of the general advances with the most impact has been the introduction of microwave synthesis techniques [152]. This has both reduced reaction times and improved reaction yields for many of the coupling and protection/deprotection reactions crucial to the synthesis of electro-optic chromophores. An example is given in figure 4. A particularly important advantage of microwave synthesis protocols over conventional reflux chemistry is the fact that the critical imine intermediate in the synthesis of cyano furan acceptors can be isolated. Such isolation permits mixed ligand

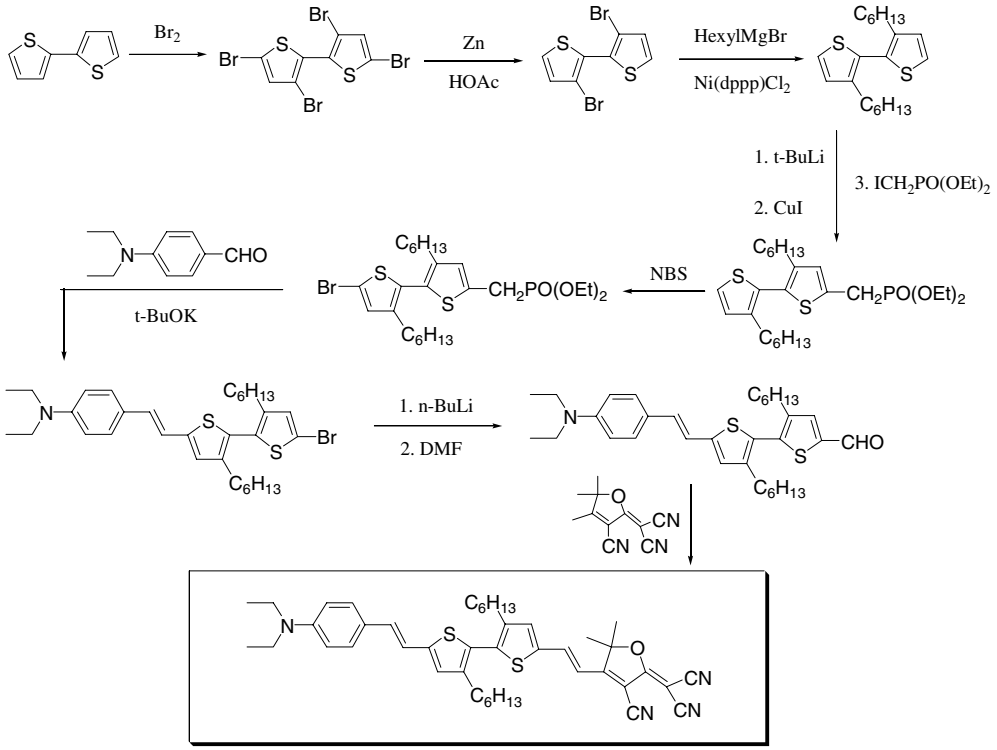

Figure 3. The synthesis of the CWC chromophore is shown. Obviously, synthesis of CLD represents a condensed version of this process.

cyano furan acceptors (such as discussed in the last section) to be prepared. The reasons why microwave synthesis techniques have been so successful are probably not fully understood at this time. Of course, microwave reactors permit very uniform heating of reaction mixtures and thus avoiding thermal gradients. Since desired primary and unwanted side reactions are likely to have different temperature dependences, uniform heating permits optimization of the desired product yield while minimizing unwanted side reaction product contamination.

In the next section, we shall see that it is not sufficient to focus on just the active pi-electron portion of electro-optic chromophores. How these chromophores are functionalized for incorporation into nanostructured materials that minimize unwanted intermolecular electrostatic interactions is critically important. The three-dimensional structures of chromophores will be important as will their functionalization and the chemical processing necessary to incorporate these materials into the desired macroscopic lattices. The exact types of chemistry required for translating chromophores into the desired macroscopic lattices will depend upon the type of final material lattice considered, e.g. composite, homopolymer, copolymer, crosslinked dendrimer, dendronized polymer. We shall defer discussion of that chemistry to a later section. However, as a general caveat, it is useful to note that absolute conclusions are dangerous. Chromophores that initially exhibit poor solubility may exhibit dramatically improved solubility with a minor modification in structure. For example, CLD chromophores without the isophorone group are difficult to process: however, addition of this group not only improves electro-optic activity by reducing unwanted electrostatic interactions that drive centrosymmetric crystallization but also improves solubility, stability and optical loss.

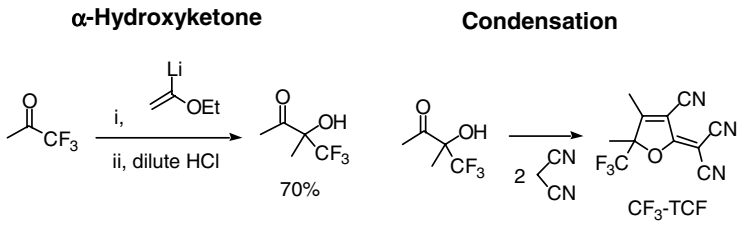

Condition	Reaction time	Yield (%)
Reflux	48 h	30
Microwave	20 min	55

Table. Comparison of conventional and microwave

Figure 4. A comparison of microwave and conventional reflux synthesis is shown.

Incorporation of chromophores into dendrimer structures can lead to significant improvements in electro-optic activity, optical loss, processability and stability [151, 153–157].

3. Macroscopic electro-optic activity

Macroscopic electro-optic coefficients are measured by techniques such as ellipsometry, attenuated total reflection, two-slit interference modulation and by utilization of various types of device structures: as measurement techniques have been reviewed elsewhere [11, 18, 26], they will not be reviewed here. The translation of exceptional molecular hyperpolarizability into macroscopic electro-optic activity is clearly the most daunting challenge in the optimization of organic electro-optic materials. Macroscopic electro-optic activity requires that the chromophores be organized into a noncentrosymmetric lattice. One or more forces will be required to drive such organization. Commonly used approaches include electric field poling of a chromophore lattice near its glass transition temperature or layer-by-layer sequential synthesis starting from a substrate surface. Opposing such noncentrosymmetric organization will be thermal forces (which promote random order of chromophores) and intermolecular electrostatic dipolar interactions (which favour centrosymmetric order). In the absence of forces that promote noncentrosymmetric order, dipolar chromophores will crystallize in centrosymmetric space groups. The few exceptions to the oft-observed centrosymmetric crystalline order are materials such as DAST [158–165] where ionic forces overwhelm dipolar interactions and drive noncentrosymmetric crystallization.

In this discussion, we limit our consideration to dipolar chromophores organized by electric field (E_p) poling of such chromophores incorporated into polymer, dendrimer or dendronized polymer structures near the glass transition temperature of the material lattice. The poling-induced order is locked in either by crosslinking (covalent bond formation) or by cooling the material to room temperature. In the latter case, the lattice stabilization will be effective only if the poling temperature is substantially above operating and subsequent processing temperatures.

Electro-optic activity, r_{33}, can be obtained by computing the noncentrosymmetric order parameter, $\langle \cos^3(\theta) \rangle$, of equation (1) by statistical mechanical methods providing the partition function incorporating all relevant potential interaction energies is appropriately specified. N is

$$r_{33} = N\langle\cos^3(\theta)\rangle\frac{2\beta f(\omega)}{n^4} \tag{1}$$

the chromophore number density, β is the molecular hyperpolarizability, n is the index of refraction and $f(\omega)$ accounts for local field factors from the dielectric nature of the environment surrounding the chromophores. Chromophore-electric poling field and thermal energies are easily specified. Indeed, in the absence of intermolecular electrostatic interactions, $\langle\cos^3(\theta)\rangle = \mu F/5\ kT$, where μ is the chromophore dipole moment, F $(=f(0)E_p)$ is the electric poling field felt by the chromophore, k is the Boltzmann constant and T is the Kelvin temperature. This explains why $\mu\beta$ values were reported throughout the 1980s and 1990s when comparing chromophores. At low chromophore concentrations, electro-optic activity will increase in a linear manner with chromophore number density, chromophore dipole moment and poling field strength. At higher concentrations, where intermolecular electrostatic interactions come into play, $\langle\cos^3(\theta)\rangle$ and N will no longer be independent and electro-optic activity will exhibit a more complex dependence on $\langle\cos^3(\theta)\rangle$, N and the poling field strength. The process of defining optimum electro-optic activity involves maximizing $N\langle\cos^3(\theta)\rangle$ for a given molecular hyperpolarizability.

In the development of electro-optic materials, two classes of materials are encountered that are amenable to quite different theoretical treatments. The first are chromophore/polymer composites. Near the glass transition temperature of such materials, the motion of the chromophore (relevant to defining the equilibrium distribution of chromophores and defined by interaction potentials and thermal energy) is, to first order, independent of the polymer host. For chromophore/polymer composite materials there are no covalent bonds between chromophores and the polymer host. The pi-electron orbital interaction inhibits chromophores from bending and twisting extensively so these can approximately be considered relatively stiff (rigid) objects. The pi-electron component of the chromophore is, to a good approximation, of prolate ellipsoidal shape. The problem of defining poling-induced order thus reduces to computing the interplay of chromophore dipole moment–electric poling field interaction, chromophore–chromophore electronic (r^6) interactions and chromophore–chromophore steric (r^{12}) interactions, in defining $\langle\cos^3(\theta)\rangle$. These interactions are all scaled by thermal energy, kT. Chromophore/polymer composite materials represent attractive model systems for the study of the process of optimizing electro-optic activity because theoretical considerations are minimized and because samples are readily prepared. For practical device applications, composite materials are less attractive. Since chromophores are not tethered to the host lattice, sublimation at high processing temperatures and electrophoretic migration under electric field poling are problems that can be encountered. Chromophores can also be extracted by spin casting solvents during deposition of cladding layers (to be discussed later). Phase separation of chromophores and polymers can be encountered and depends upon both chromophore concentration and processing conditions. Relaxation of poling-induced electro-optic activity by chromophore orientation is generally more problematic with composites due to the absence of coupling (other than steric interaction) of the chromophore and the polymer host.

The second class of materials involves covalent bond coupling of electro-optic chromophores to a macromolecular material lattice. Extreme examples of this class of electro-optic materials are chromophore-containing dendrimers and dendronized polymers. With such materials, the chromophore is essentially surrounded by 'host' material and covalently coupled at several points to the host lattice. Obviously, chromophore motion will not be independent of the host material and covalent bond potentials must be taken into account in computing order parameters. Theoretical techniques, such as atomistic Monte Carlo calculations [166], are more appropriate for this class of materials. Chromophore lattices formed by layer-by-layer deposition techniques also fall into this category.

We now turn to considering the use of statistical mechanics in defining structure/function relationships necessary for optimizing electro-optic activity for these two classes of organic electro-optic materials.

3.1. Theory of chromophores/polymer composites

For concentrations of electro-optic chromophores dissolved in flexible chain polymers sufficiently low that aggregation is not a problem, the fluid phase that exists near the glass transition temperature can be viewed as rigid-object chromophores diffusing in a medium of uniform and isotropic dielectric constant and viscosity. The pi-electron system of the chromophore ensures a rather long persistence length so that one does not have to worry about a large number of molecular conformations. Moreover, it is reasonable to assume that, for these conditions, an equilibrium distribution of chromophore orientations will exist, i.e. the distribution can be described by equilibrium statistical mechanical methods. In other words, we do not have to worry about the details of the dynamics of chromophore reorientation under the poling field. We shall later learn from Monte Carlo calculations that this is not a good approximation for all samples of interest. Indeed, atomistic and modified atomistic kinetic Monte Carlo calculations will be necessary to describe the behaviour of some samples (e.g. those with high chromophore concentrations and for multi-chromophore-containing dendrimer structures). However, as we shall shortly demonstrate, a simple model of rigid chromophores freely reorienting in an isotropic medium has the great advantage of permitting analytical expressions for electro-optic activity as a function of chromophore concentration to be derived and of permitting the evaluation of the effect of chromophore shape on electro-optic activity using numerical algorithms [167–172].

We have shown that, within the framework of this simple model, that three factors influence poling efficiency and hence electro-optic activity: (1) the chromophore dipole moment (μ)–electric poling field (F) interaction; (2) intermolecular electrostatic interactions among the high dipole moment chromophores; and (3) thermal energy (molecular collisions). For electric poling field strengths typically used (e.g. >100 V μm^{-1}), intermolecular electrostatic interactions will not make an important contribution for concentrations of normal interest (<45 wt/wt%) for chromophores with dipole moments of 7 D or less. However, most chromophores of interest for device fabrication exhibit dipole moments of 10–18 D. The problem thus becomes one of defining the electric field felt by a reference chromophore from an ensemble of surrounding chromophores. This field reflects a many-body interaction and long-range cooperativity among chromophores; a simple two-body interaction picture is inadequate. Piekara [173, 174] viewed this problem as introducing a potential function describing a dipole embedded in a 'crystallite' of surrounding chromophores. With this picture, one must consider a rotation matrix that relates the reference chromophore to the poling field (laboratory) axis, a rotation matrix that relates the reference chromophore to the crystallite axis and a rotation matrix that relates the crystallite axis to the poling field (laboratory) axis. Of course, trigonometry tells us that only two of these rotation matrices are independent. With this brief introduction let us consider the development of analytical expressions taking into account the above-mentioned electronic interactions.

The mean distance between chromophores, $\bar{r}$, is related to chromophore number density, N, as $N = 1/\bar{r}^3$. In general, statistical mechanics provides the method of computing the mean order from the M particle energy, $U(r, \Omega(M), E_p)$, including a uniform electric poling field, E_p. Here $r(M)$ are the M centres of the chromophores and $\Omega(M)$ are the two (or three) Euler angles that define the spatial orientations of the M chromophores. The order parameter can be

computed from a consideration of all interactions contributing to the total energy according to

$$\langle \cos^n(\theta)\rangle = \frac{1}{M}\sum_{j=1}^{M}\int \cos^n(\theta_j)G(r,\Omega,E_p)\,\mathrm{d}r^M\,\mathrm{d}\Omega^M \Big/ \int G(r,\Omega,E_p)\,\mathrm{d}r^M\,\mathrm{d}\Omega^M \tag{2}$$

where $G(r,\Omega,E_p) = \mathrm{e}^{-U(r,(M),\Omega(M),E_p)/kT}$ is the M-particle partition function and kT is the thermal energy. θ_j is the angle of the jth dipole to the poling field. From an analytic perspective, this is a difficult problem. To make progress we suggest that a single chromophore, 1, be designated as the one for which the averaging is done. Then we can average over all other chromophores. The non-normalized probability distribution around the first one is then $P_M(\Omega_1)$, where $P_M(\Omega_1) = \int G(r,\Omega,E_p)\,\mathrm{d}r^M\,\mathrm{d}\Omega^{M-1}$. Then the average order is $\langle\cos^n(\theta_1)\rangle = \int_{\Omega_1}\cos^n(\theta_1)P_M(\Omega_1)\,\mathrm{d}\Omega_1/\int_{\Omega_1}P_M(\Omega_1)\,\mathrm{d}\Omega_1$. Here, we deviate from the standard statistical mechanical treatment and follow Piekara [173, 174], who suggested that the bulk material consists of many solidus regions that cannot inter-convert. The orientation θ_1 (or Ω_1), relating chromophore 1 to the laboratory frame, may be considered to be composed of two rotations. The first is a rotation from the laboratory frame to a centre of local symmetry of the particular region of the amorphous solid that defines a local axis of symmetry, θ (or Ω), and the second rotation is that from the centre of symmetry to the orientation of chromophore 1 in the local potential field due to all the other chromophores. The angle of deviation from the local symmetry axis is $\theta_{\bar{M}}$ (or $\Omega_{\bar{M}}$): $\theta_1 = \theta + \theta_{\bar{M}}$, which is rigorously true when the minor angles are equal. More generally, the Euler angles are related formally as $\Omega_1 = \Omega \oplus \Omega_{\bar{M}}$. Thus, the angle θ_1 is related to the other Euler angles by $\cos(\theta_1) = \cos(\theta)\cos(\theta_{\bar{M}}) + \sin(\theta)\sin(\theta_{\bar{M}})\cos(\phi - \phi_{\bar{M}})$. In Piekara's approach [173, 174] the above statistical integral is done in two parts. $P_M(\Omega_1)$ is replaced by a $P_{\bar{M}}(\Omega_1)$, the local distribution function referenced to a single soldius crystallite region. An additional averaging is then necessary over a uniform distribution of soldius regions. All the while, chromophore 1 must interact with the poling field. Therefore, the averaging over the orientations of 1 must be done in two steps. The first is the averaging over the effective field around the centre of symmetry for a single crystallite region. Therefore

$$\langle \cos^n(\theta)\rangle_{\bar{M}} = \frac{\int_{\Omega_{\bar{M}}}\cos^n(\theta_1)P_{\bar{M}}(\Omega_1)\,\mathrm{d}\Omega_{\bar{M}}}{\int_{\Omega_{\bar{M}}}P_{\bar{M}}(\Omega_1)\,\mathrm{d}\Omega_{\bar{M}}}. \tag{3}$$

This average must then be averaged over all crystallites, in terms of Ω:

$$\langle \cos^n(\theta)\rangle = \frac{1}{8\pi^2}\int_{\Omega}\langle\cos^n(\theta)\rangle_{\bar{M}}\,\mathrm{d}\Omega. \tag{4}$$

Piekara [173, 174] suggested a specific form for $P_{\bar{M}}(\theta_1)$ as: $P_{\bar{M}}(\theta_1) = \frac{1}{4\pi}\mathrm{e}^{-f\cos\theta_1}\mathrm{e}^{-w\cos\theta_{\bar{M}}}$, where w is an undetermined constant, independent of the poling field, and $f = E_p\mu/\varepsilon kT$. The first term $\mathrm{e}^{-f\cos\theta_1}$ is due to the poling field acting on chromophore 1 and the second term $\mathrm{e}^{-w\cos\theta_{\bar{M}}}$ is the leading term in an expansion of the effect of all other chromophores in the vicinity of chromophore 1. With this definition of the single-particle probability distribution, we can evaluate the following integral:

$$\begin{aligned} G(z) = \frac{\sinh(z)}{z} &= \frac{1}{4\pi}\int_{\cos(\theta_{\bar{M}})=-1}^{1}\int_{\phi_{\bar{M}}=0}^{2\pi}\mathrm{e}^{\{-f\cos\theta_1\}}\mathrm{e}^{\{-w\cos\theta_{\bar{M}}\}}\,\mathrm{d}\cos\,\theta_{\bar{M}}\,\mathrm{d}\phi_{\bar{M}} \\ &= \int_{\Omega_{\bar{M}}}P_{\bar{M}}(\Omega_1)\,\mathrm{d}\Omega_{\bar{M}} \end{aligned} \tag{5}$$

where $G(z)$ is the generating function then for the rest of the integration. Moreover, z is just the magnitude of the vector sum of the poling field and the local crystal field:

$$z^2 = f^2 + w^2 + 2fw\cos(\theta). \tag{6}$$

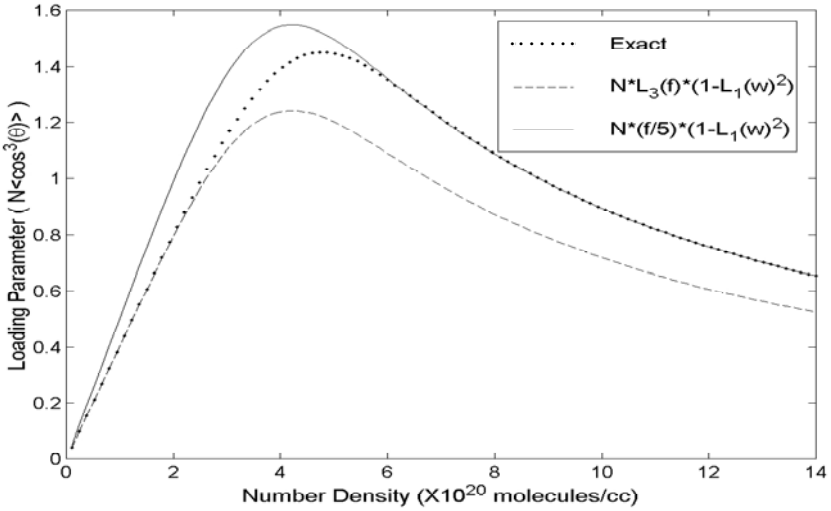

Figure 5. Variation of the loading parameter with chromophore number density for calculations discussed in the text is shown.

This result demonstrates the vector nature of the interaction of the local crystallite field and the poling field on the individual chromophore. The poling field–dipole interaction energy of the simple Langevin theory is now replaced with the interaction energy, which consists of the vector sum of the local interaction field with the poling field. The final averaged quantity of interest can then be determined using the generating function:

$$\langle \cos^n(\theta) \rangle = \frac{1}{2} \int_{\cos(\theta)=-1}^{1} \frac{1}{G(z)} \frac{\partial^n G(z)}{\partial^n f} \, \mathrm{d}\cos\theta. \tag{7}$$

The integrand can be evaluated and written as an analytic function of z. The integrand can be written in terms of the first Langevin function, $L(z)$, with z as its argument:

$$L(z) = \coth(z) - \frac{1}{z}. \tag{8}$$

The integral for the case of $n = 3$ is

$$\langle \cos^3(\theta) \rangle = \frac{1}{2} \int_{\cos(\theta)=-1}^{1} (f + w\cos(\theta)) \left[3 \left\{ \frac{3\frac{1}{z}L(z) - 1}{z^2} \right\} + (f + w\cos(\theta))^2 \left\{ \frac{5 - (z^2 + 15)\frac{1}{z}L(z)}{z^4} \right\} \right] \mathrm{d}\cos\theta. \tag{9}$$

Here the two groupings of $L(z)$ make the functional forms numerically stable at small z. This integral may be numerically evaluated in this form. The integrand is analytic and finite everywhere.

The electro-optic coefficient is then proportional to the loading parameter, defined as $\mathrm{LP}(N) = N\langle \cos^3(\theta) \rangle$. To plot the loading parameter as a function of N, we now assume a form for the dependence of w on N that we will later show is supported by the Monte Carlo calculations: $w = \left(\frac{\mu^2}{r^3 kT}\right)^2 = \left(\frac{N\mu^2}{kT}\right)^2$. The loading parameter, as a function of the chromophore density, N, is shown in figure 5. Superimposed are the approximate expressions for the loading parameter, previously developed [167]. The first approximation, obtained when the poling

field is small compared to the thermal energy, is $\langle\cos^n(\theta)\rangle = \frac{f}{n+2}\{1 - L_1^2(w)\}$. The second approximation is a modification of the first that limits to the correct, third-order, Langevin function at low w (or low N): $\langle\cos^n(\theta)\rangle = L_n(f)\{1 - L_1^2(w)\}$, valid for $n = 1$ or 3. The two approximations everywhere bound the correct value of the loading parameter. Note that the value of chromophore loading density at which the maximum electro-optic activity occurs differs somewhat from the value given by the two approximations. The approximate relations depend on the loading density through an attenuation factor, which itself depends only on local interaction energy (w) and hence upon N. The maximum loading is an analytic function of w and is found when $\frac{w}{\langle\cos\theta\rangle}\frac{\partial\langle\cos\theta\rangle}{\partial w}\big|_{w=w_{max}} = -\frac{1}{2}$. From this analytic expression, one may easily prove that the maximal loading density is determined by a condition on w, and is a function of f. When $f \ll 2$, the maximum in the loading function occurs when

$$w_{max} = \left(\frac{\mu^2 N_{max}}{kT}\right)^2_{f=0} = 1.9139 \tag{10}$$

from which N_{max} is readily calculated, i.e. $N_{max} = 1.38kT/\mu^2$. The general dependence of w_{max} on f is well approximated by the expression

$$w_{max} \simeq 0.9139 + \sqrt{1 + \left(\frac{f}{2}\right)^2}. \tag{11}$$

The value of N_{max} may be determined from this universal function after the dipole moment is specified.

In the simplest treatment, the effects of the shape of the chromophore may be considered as the interaction of two hard-sphere ellipsoids separated by a distance $\bar{r}$. The mean intermolecular distance is determined from the number density, as given above. However, if the ellipsoids are prolate then they both cannot point along the line joining their centres if the concentration is in a region where $2a > \bar{r} > 2b$, where a and b are the major and minor semi-axes of the prolate ellipsoid. In this regime, there is a constraint on the angles accessible to an ellipsoid before colliding with a neighbour (at the same orientation). The orientation of the molecule is found from the x and y distances from the centre to the surface: $x^2 + y^2 = (r/2)^2$. The equation for the surface of the ellipse is $\left(\frac{x}{b}\right)^2 + \left(\frac{y}{a}\right)^2 = 1$. From these two equations and two unknowns the cut-off (or the minimum angle that can be accessed) as a function of $\bar{r}$ is $c = c(\bar{r}) = \cos(\theta_{min}) = 1 - (2b/\bar{r})^2/1 - (b/a)^2$. A similar expression is found for the oblate ellipsoid case. The cut-off function, $c(\bar{r})$, is a continuous function of $\bar{r}$ or N, because $c(\bar{r}) = 1$ for $\bar{r} > 2a$ and $c(\bar{r}) = 0$ for $2b > \bar{r}$. This minimum angle can be incorporated into the evaluation of the order parameters by restricting the limits of integration so that $-c \leqslant \cos(\theta_M) \leqslant c$. The effect of the prolate (or oblate) ellipsoids is to restrict the ordinates the chromophore can access. Therefore, we suggest that the local crystallite-orienting field be restricted in both angular directions. Therefore the generating function for the ellipsoid is

$$G_E(z) = \frac{1}{2cc'}\int_{\cos(\theta_{\tilde{M}})=-c}^{c}\int_{\phi_{\tilde{M}}=0}^{c'} \mathrm{e}^{\{-f\cos\theta_1\}}\mathrm{e}^{\{-w\cos\theta_{\tilde{M}}\}}\,\mathrm{d}\cos\,\theta_{\tilde{M}}\,\mathrm{d}\phi_{\tilde{M}}. \tag{12}$$

This double integral is quite difficult, and can be done numerically. However, to obtain some insight we have done the phi integral and carried it to the limit of maximum cut-off. At this point there is only a single direction in phi toward which the dipole can point. Using this limiting form, the generating function may be expanded in Bessel functions, which gives a quick evaluation of the integral. The mean order parameter is found in the same way:

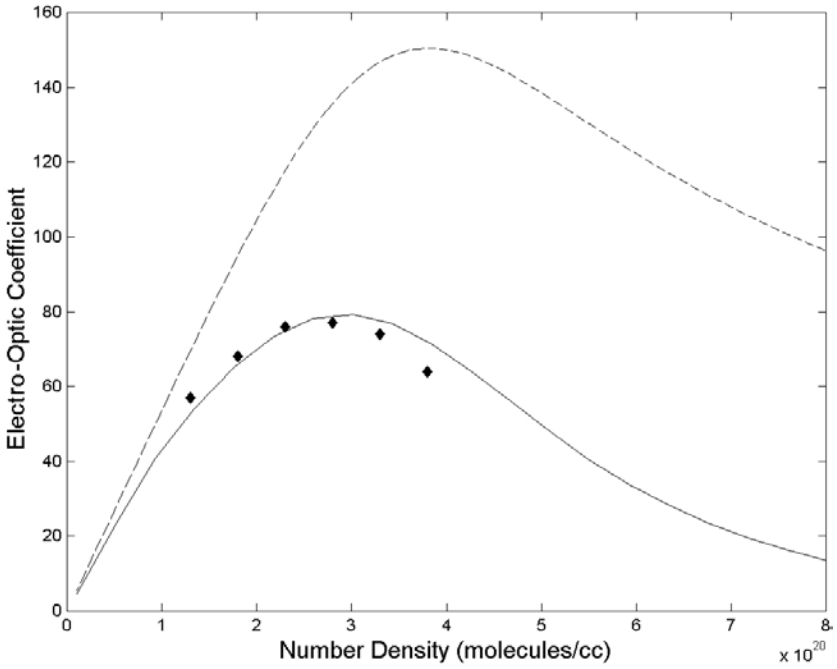

Figure 6. Comparison of experimental data (full symbols) for a CLD chromophore/APC polymer composite with theoretical calculations assuming prolate ellipsoidal (full curve) and spherical (broken curve) chromophore shapes is shown.

$$\langle \cos^n(\theta) \rangle = \frac{1}{2} \int_{\cos(\theta)=-1}^{1} \frac{1}{G(cz)} \frac{\partial^n G(cz)}{\partial^n f} \, \mathrm{d}\cos\theta. \tag{13}$$

The following figure shows the effect of using the major and minor axes of one of the chromophores and comparing the calculation for the case of a spherical chromophore with that of an ellipsoidal chromophore. Results are shown in figure 6 and compared with experimental data. The remarkable improvement in agreement with the data is obtained with no adjustable parameters.

We have also carried out Monte Carlo computational analysis [170] of the competition of electric field poling and intermolecular electrostatic interactions in determining order parameters. The comparison of Monte Carlo defined potential functions with the analytical approximation described here is shown in figure 7 [170]. The good agreement argues strongly for the reasonableness of our choice of w in our analytical approach.

For chromophores physically incorporated into polymers, such as poly(methylmethacrylate) (PMMA) or amorphous poly(carbonate) (APC), to form composite materials, the theory just discussed provides quantitative guidance for the design of chromophores and processing conditions. It is very gratifying that numerical calculations run on a personal computer can be used to define the concentration of chromophores leading to maximum electro-optic activity and the optimum poling conditions. Moreover, when combined with quantum mechanical structure optimization calculations, simple theory can be used to systematically guide the design of improved chromophores. The simple theory described has dramatically reduced the Edisonian nature of the development of improved electro-optic materials and has led to the rapid improvement in electro-optic activity demonstrated over the past several years [42, 167–172]. The obvious simple design paradigm is to make chromophores more rotund.

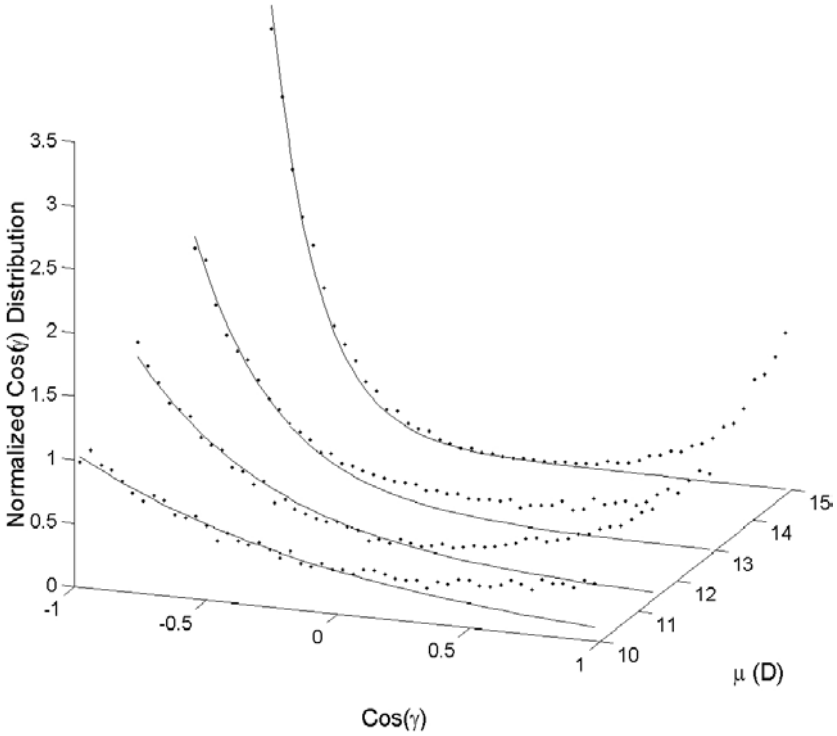

Figure 7. A comparison of analytic (curves) and Monte Carlo derived (symbols) intermolecular electrostatic potential functions is shown. The left-hand side corresponds to the potential for centrosymmetric ordering while the right-hand side reflects noncentrosymmetric ordering potential.

3.2. Theory of chromophores covalently coupled to various supramolecular structures

While electro-optic activity can be improved somewhat by relatively simple derivatization of chromophores to prevent their close approach along their minor axes (this approach is particularly problematic for favouring centrosymmetric organization and indeed is a critical step in centrosymmetric crystallization), this modification paradigm has limitations which are obvious from considering the theoretical calculations discussed in the preceding section [11, 26, 42, 167–172]. Derivatizaton has most commonly taken the form of the addition of simple alkyl or alicyclic groups. Even though the amount of steric hindrance is modest, improvement in electro-optic activity approaching factors of two has been realized. Such modifications have the added advantage of improving chromophore/spin casting solvent interactions (hence solubility and processability) and the compatibility of chromophores with organic host polymers. In some cases, even chemical stability has been improved.

However, such modifications do not place restrictions on chromophore motion with respect to the host lattice and thus miss additional opportunities to engineer the desired noncentrosymmetric order. Early research on multi-chromophore-containing dendrimers [151] showed that electro-optic activity for a chromophore could be doubled (to 60 pm V^{-1} at 1.55 μm) from the best value obtained for a chromophore/polymer composite by incorporating the chromophore into a multi-chromophore dendrimer. The TS of electro-optic activity was also significantly improved by this incorporation. The dendrimer in question involved the incorporation of three chromophores. The focal point of the dendrimer was a rigid group with

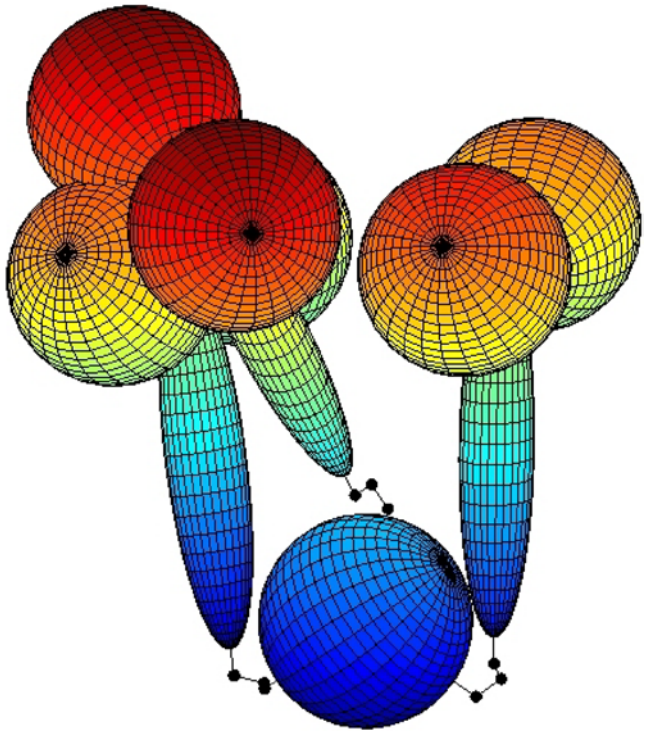

Figure 8. The Monte Carlo computed conformation of a three-chromophore dendrimer in an electrical poling field is shown. Each chromophore is assumed to be characterized by a dipole moment of 15 D. Full van der Waal's interactions are considered.

three relatively short flexible arms extending to make an attachment to the three relatively rigid chromophores. From the terminal ends of each of the three chromophores are attached two relatively rigid moieties. The detailed chemical structure of the multi-chromophore dendrimer is given in [151] but a reasonable first-order theoretical model is shown in figure 8. This model reproduces the essential features of the experimental data although the reader should be cautioned that no direct structural information exists at this time. The electric poling field induced structure calculated by pseudo-atomistic Monte Carlo results (only the flexible chain segments are treated in a fully atomistic manner while the rigid segments are treated approximately as described above) are shown in figure 8. With the poling field turned off, the chromophores lie roughly in a triangular plane (in an approximate head-to-tail conformation). This clearly represents a minimum energy configuration driven by dipole–dipole interactions. This conformation resembles an open umbrella. The effect of the poling field is to close the umbrella or to invert the umbrella (into a closed conformation) depending on the length of the flexible chain spacer. The closed umbrella conformations are subsequently locked in place by chemical crosslinking. Both theory and experiment suggest that there is relatively little interpenetration of dendrimers—thin films of the dendritic materials crack readily unless they are crosslinked but the cracks heal upon heating. This is suggestive of weak inter-dendrimer forces. It is the crosslinking that accounts for the exceptional TS.

The importance of developing pseudo-atomistic Monte Carlo simulations, that can take into account critical bond potentials but at the same time be executed with a reasonable expenditure of computer time and power is illustrated by figure 8. This relatively simple model

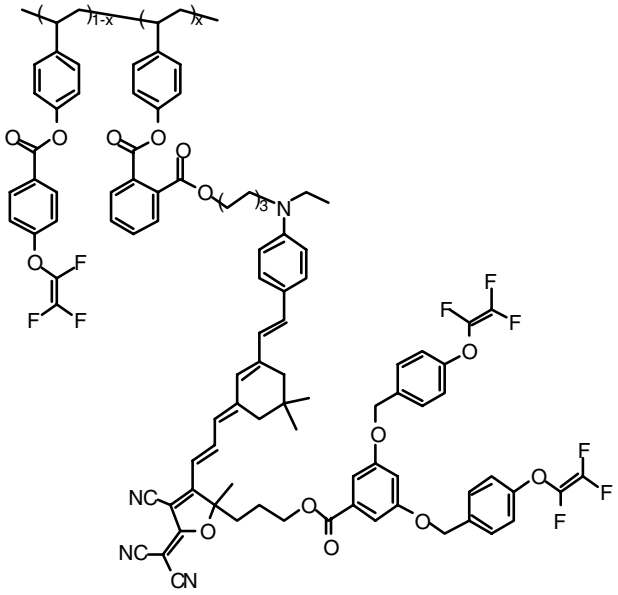

Figure 9. The molecular structure of a dendronized polymer is shown.

appears to provide a useful insight into the design of complex structures and calculations can be executed on a variety of structural variants. Hopefully, it will permit theory to move from the role of simply rationalizing experimental results to suggesting new structures to be synthesized. Unfortunately, this is not yet the case, as is illustrated by our next example of complex nanostructured electro-optic material architectures. Not only can electro-optic chromophores be incorporated into single-chromophore dendrimers [175] and multi-chromophore dendrimers [151, 155–157] but they can also be incorporated into dendronized polymers [176]. Such dendronized polymers may form tobacco mosaic virus type structures as demonstrated by Percec [177–179]. Such dendronized polymer structures may lead to chromophores aligned in a spiralling helix. Two materials that may be amenable to dendronized polymer structure formation are shown in figures 9 and 10. When the CLD chromophore (see figures 9 and 10) are used with these structures, electro-optic coefficients of 97 and 111 pm V^{-1} are obtained. This is to be compared to a value of 58 pm V^{-1} for CLD physically incorporated into a polymer composite. Improvements in electro-optic activity of nearly a factor of two are achieved that can be associated with spatial control of chromophore–chromophore intermolecular electrostatic interactions. Unfortunately, neither structural characterization nor theoretical data exist to give a precise picture of the 3D architecture of such dendronized polymers but such data should be forthcoming from new theoretical methods. Dendronized polymers also facilitate the realization of excellent TS of electro-optic activity. Little or no decay of electro-optic activity occurs even at a temperature of 85 °C even over periods of 1000 h.

If the linear behaviour of electro-optic activity as a function of chromophore number density could be maintained by eliminating electrostatically driven centrosymmetric ordering, electro-optic activity in excess of 1000 pm V^{-1} could be obtained. With the advances in chromophore hyperpolarizability that are currently being realized, together with improved architecture control achieved through nanostructural engineering, it should be possible to obtain electro-optic coefficients an order of magnitude greater than the 32 pm V^{-1} currently realized for lithium niobate.

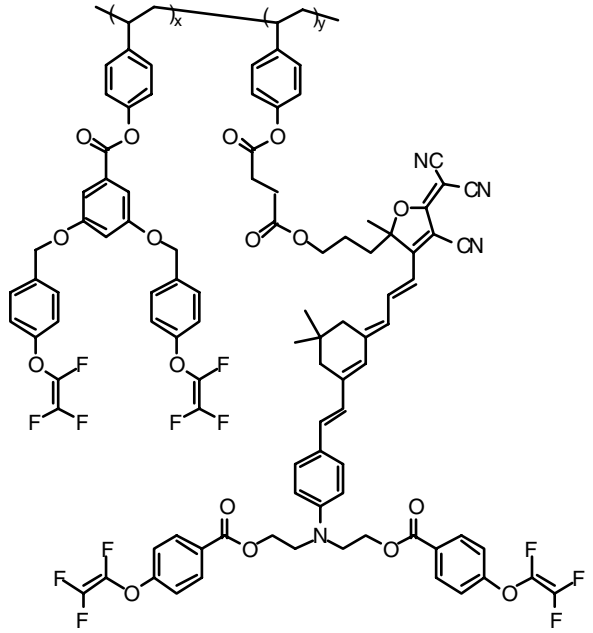

Figure 10. The molecular structure of a second dendronized polymer is shown.

3.3. Electric field poling and lattice hardening

Noncentrocentrosymmetric order in electro-optic materials is most commonly achieved by electric field poling techniques, ranging from corona poling to a variety of electrode poling protocols [11, 18, 26, 57] including pulsed poling methods [180]. As these have been discussed in the cited references, we will not discuss poling configurations further here other than to comment that pulse poling techniques [180] appear to be an effective route to disrupting centrosymmetric crystallization that occurs with high dipole moment chromophores in the absence of a poling field (e.g. during spin casting). Pulsed poling appears to permit high fields to be obtained without inducing dielectric breakdown that would occur if such fields were applied continuously. As already noted, it is convenient to monitor *in situ* the induction of nanocentrosymmetric order by electric field poling. This is conveniently done using detection of second harmonic generation [10] (see figure 11). Also, conductivity of active electro-optic materials (and thus the presence of ionic impurities) will play an important role in defining poling efficiency; thus, monitoring electrical conductivity can also prove useful [26]. A convenient means of studying the electric field dependence of poling-induced order is the 'constant bias' technique [181–183]. This is basically a Mach–Zehnder or birefringent modulator device structure operated under a constant bias (poling field) at elevated temperature. When electrode poling through cladding layers is carried out, the conductivity of the cladding is a critical factor in determining the field felt by the chromophores. Use of conducting cladding layers has been discussed in several papers by Grote and coworkers [184–190]. While conducting cladding layers permit the electric field to be dropped across the cladding layers thus increasing the poling field felt by the chromophores in the active layer, conducting cladding materials have typically been characterized by high optical loss. Indeed, these layers can dominate waveguide loss from the effect of optical fields fringing into the cladding layers. Another problem associated with conducting claddings is the frequency dependence

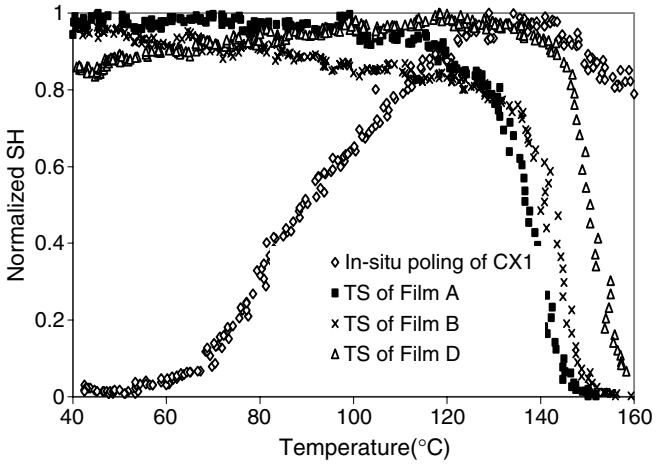

Figure 11. The use of second harmonic generation detection to monitor the induction of second-order optical nonlinearity by electric field poling (diamonds) and the TS of poling-induced optical nonlinearity with heating is illustrated. The sample is crosslinked CLD utilizing the TFVE crosslinking reagent [209].

of conductivity, which causes V_{pi} to increase with increasing frequency. Use of conducting claddings is an activity that clearly requires more research.

A fundamental dilemma faced in the preparation of device quality electro-optic materials is that one would like to carry out spin casting and poling at modest temperatures to avoid chromophore or host material decomposition and yet end up with a high glass transition material lattice that locks-in poling-induced noncentrosymmetric order. Thus a great deal of research effort, particularly in the period 1990–1995 [18, 52, 57], has been focused on methods of hardening (crosslinking) material lattices during electric field poling [191–209]. Approaches to the problem of achieving a 'hard' lattice have focused on either covalent coupling of a chromophore to a high glass transition polymer (where the glass transition temperature is defined by the segmental flexibility) or by crosslinking during the electric field poling process [18, 52, 57]. The problem with the former approach is that high processing temperatures (defined by the glass transition temperature of the polymer) are required and thus the chromophore must withstand such temperatures. Also, high glass transition polymers have, in general, exhibited poor solubility in traditional spin casting solvents and it has been difficult to obtain optical quality thin films for such materials. Of course, the problems of chromophore sublimation and diffusion are suppressed by covalent coupling to the polymer backbone. Later in this discussion, we will deal with one example where covalent coupling to a high glass transition polymer yields a material simultaneously characterized by large electro-optic activity and good TS [209].

Most of our discussion will focus on materials where the glass transition is elevated by crosslinking during the electric field poling process. Two general approaches to crosslinking have been pursued in the past: these are photo-induced and thermal-induced crosslinking [18]. Of the two, photocrosslinking has, to this point in time, proven unsuccessful in yielding lattices with adequate hardness. The obvious reason for failure is that much of the ultraviolet (UV) or visible wavelength light directed toward the photo-initiator is absorbed by the electro-optic chromophores. UV and visible wavelength light could conceivably promote chromophore decomposition if applied for sufficient time: however, in practice this does not appear to be

a general problem. Indeed, UV-curable epoxies are routinely used as cladding materials and the active electro-optic layer experiences considerable exposure in the processing of curing cladding materials. The problem of absorption of light by electro-optic chromophores could conceivably be avoided by using near-infrared (beyond 1.3 μm wavelength) light and a two-photon photo-initiator. This appears not to have been achieved, or perhaps not even explored, at this point in time.

All practical crosslinked electro-optic materials have been achieved by thermally induced crosslinking. A fundamental problem with this approach is that both of the processes that must be reconciled (electric field poling and crosslinking) are dependent upon temperature and the temperature dependences must therefore be compatible. In short, considerable thought must be given to the selection of poling and lattice hardening protocols. Some industrial research groups believe that such sophistication is incompatible with industrial manufacturing and thus choose not to consider crosslinkable materials. However, at present, crosslinked electro-optic materials have proven the most realistic for development and evaluation of prototype devices so work has continued in this area. Clearly, it is incumbent upon the organic chemist to develop the most straightforward and problem-free lattice hardening chemistries if materials are to be adopted commercially. Poling and crosslinking must occur in the same temperature regions with crosslinking ideally occurring at somewhat higher temperatures. At a given temperature, one would also desire that the kinetics of chromophore reorientation (rotational diffusion) under the influence of the poling field be faster than the kinetics of crosslinking. Because optical quality materials are essential, it is in general not possible to use catalysts to control the rate of the crosslinking reaction. Thus, finding crosslinking reactions with the right temperature-dependent kinetics is essential. Of course, various levels of sophistication have been demonstrated, including the use of two different crosslinking reactions and the use of novel reversible crosslinking reactions based on the reverse Diels–Alder reaction (as will be discussed shortly).

Once a thermally activated crosslinking reaction has been identified, stepped poling protocols (where electric field strength and temperature are increased periodically as a function of time) have proven very useful in optimizing both electro-optic activity and TS [18]. Obviously, with a stepped protocol lattice hardness is increasing with time as the crosslinking reaction progressively occurs: thus the electric field can be increased in time without risk of dielectric breakdown (damage to the electro-optic material). The stepped protocol keeps the crosslinking reaction from accelerating and locking up the lattice before effective chromophore reorientation, under the influence of the poling field, can occur. In some cases, stepped poling protocols permit electro-optic activity to be doubled relative to that obtained with optimized single-step protocols. Indeed, in some cases little attenuation in electro-optic activity for hardened materials is observed relative to that for the same chromophore in a guest/host composite. Without attention to detail, significant (factors of 2 or 3) reduction in poling efficiency is frequently observed. Computer control and *in situ* monitoring of stepped poling protocols are critical to successfully transitioning this processing to engineering and manufacturing environments.

Thermally induced crosslinking reactions can be further classified as reactions based on the growth of oligomers (such as in urethane or sol–gel chemistries) and the crosslinking of polymeric precursors ([11, 18, 52, 57] and references cited therein). Urethane crosslinking chemistry has been extensively investigated [191] and we now review the critical conclusions of that work. Like sol–gel reactions [18], urethane chemistry is based on condensation to yield water as a reaction product; thus, these reactions are inherently sensitive to moisture. Like sol–gel chemistry, urethane chemistry involves the growth of oligomers. At any stage of the reaction, the reaction mixture is inherently inhomogeneous containing oligomers of

different sizes and chemical composition [191]. Unless reaction stoichiometries and kinetics are carefully controlled, oligomers that are incompatible can arise and phase-separate, leading to materials with unacceptably high optical loss. Because of the sensitivity of OH and NCO reagents to atmospheric moisture, water in the air can upset reaction stoichiometry and lead to 'cloudy' films. The optimization of urethane lattice hardening chemistry has been discussed in [191] and, when followed, can lead to device quality materials. Nevertheless, moisture sensitivity is to be avoided if possible and this problem has motivated the search for alternative crosslinking chemistries. A new crosslinking moiety that has shown considerable promise and attracted significant interest is the trifluorovinyl ether (TFVE) group that leads to perfluorocyclobutane type polymers [151, 210, 211]. This reaction pathway avoids sensitivity to atmospheric moisture and, because of the increased fluorine content (reduced hydrogen content), leads to lower absorption loss at 1.3 and 1.55 μm than other hardening schemes. Materials are routinely obtained that exhibit long-term stability of electro-optic activity at 85 °C. It has been used with a variety of material architectures ranging from oligomers, to side chain polymers, to dendrimers, to dendronized polymers. This crosslinking protocol has been adapted to the CLD chromophore by Zhang [209] and relevant data are reproduced in figure 11. The work of Zhang illustrates the general observation that the exact TS achieved will depend upon the details of the individual system (segmental flexibility of various components), intermolecular interactions and exact processing conditions. In particular, the work of Zhang suggests that the crosslinking reaction involving TFVE is catalyzed by singlet oxygen chemistry: thus less effective crosslinking is achieved when samples are poled under a nitrogen atmosphere [209]. Since some chromophores, like CLD, are more sensitive to singlet oxygen photodegradation this results in somewhat of a dilemma. The likely answer is that chromophores need to be poled and crosslinked in the presence of oxygen if the FTVE-induced lattice hardening is to be optimized but exact protocols must be adjusted for each system as singlet oxygen sensitivity will vary from system to system. For the case of CLD, Zhang has chosen instead to develop side chain polymers with controlled segmental flexibility [209]. He has obtained materials that exhibit dynamic TS to somewhat above 200 °C. More commonly TS similar to that obtained for TFVE-crosslinked CLD is obtained (figures 13 and 14). These materials exhibit electro-optic activity and optical loss values (see figure 15) very similar to those obtained for CLD/APC polymer composites. For both side chain and composite materials, electro-optic activity is still considerably attenuated by unwanted intermolecular electrostatic interactions so electro-optic coefficients are only roughly twice that of lithium niobate and a factor of two smaller than obtained with dendronized polymers.

Recently, Jen and co-workers [212] have begun exploration of reverse Diels–Alder chemistry as a method of improving lattice hardness. The concept is that of a reversible crosslinking reaction where the material de-polymerizes at an elevated temperature (the poling temperature) and then re-polymerizes as the material is cooled. When coupled with a second thermally induced crosslinking reaction this provides a means of adding additional hardness to the electro-optic material. In summary, significant progress has been made with respect to obtaining hardened electro-optic materials and current materials can likely meet Telacordia standards. However, an ideal material or ideal lattice hardening protocol has yet to be realized. This will continue to be an area of active research.

Hardened materials are also relevant to the more complex subject of photostability of organic electro-optic materials. Stegeman and co-workers [213–215] have studied photostability of a number of chromophores dissolved in soft polymer matrices. These studies were carried out in the presence of oxygen and detection was effected by monitoring the

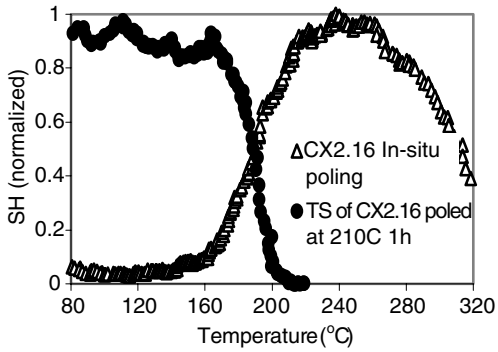

Figure 12. Induction of noncentrosymmetric order by electric field poling is monitored by second harmonic generation (triangles) as is the dynamic TS (circles). The sample is a side chain polymer material containing the CLD chromophores [209].

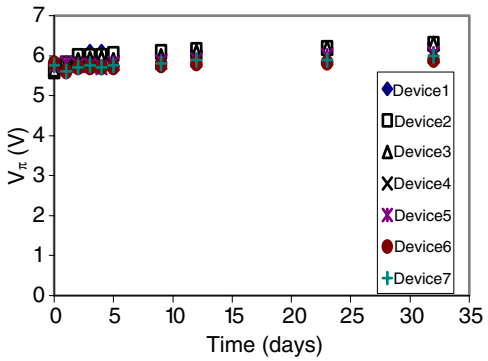

Figure 13. The stability at 85 °C of electro-optic Mach–Zehnder modulators fabricated from the organic electro-optic material of figure 12 is shown. This also illustrates the reproducibility of modulator performance from one device to the next [209].

intensity of the interband electronic transition in these charge transfer chromophores[2]. While these studies are highly worthwhile in raising the prospect that photochemical stability is an issue that needs to be addressed, the studies provide little in the way of mechanistic insights. Based on knowledge from studies of a wide range of organic, including biological, materials, it is probably safe to assume that the problem of photochemical stability is related to singlet oxygen chemistry. For example, a number of studies show that photostability improves dramatically if materials are tested under an inert gas atmosphere or hardened materials are utilized [35, 132, 216]. Indeed, it may be that simple packaging is the answer to achieving the photostability required for commercial utilization. However, design of chromophores to eliminate or sterically protect sites of potential singlet oxygen attack also influences photostability as does the presence of singlet oxygen scavengers as shown in figure 15 [216]. Lee [216] has investigated a number of chromophores and types of scavengers; his results suggest that the incorporation of scavengers could significantly improve photostability, providing other conditions are met. Figure 15 illustrates the

[2] Unfortunately, there is the possibility that the observing power could influence experimental results in the present case due to the long measurement times and due to the slow decomposition kinetics for pumping at infrared wavelengths.

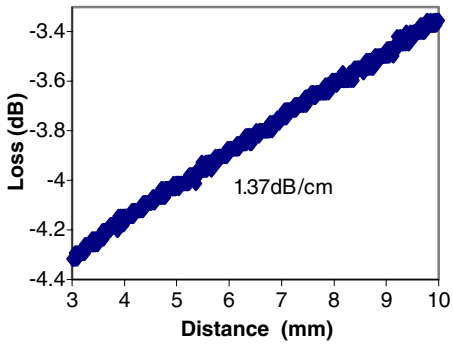

Figure 14. Measurement of optical loss by the Teng immersion technique is shown for the material of figure 12 [209].

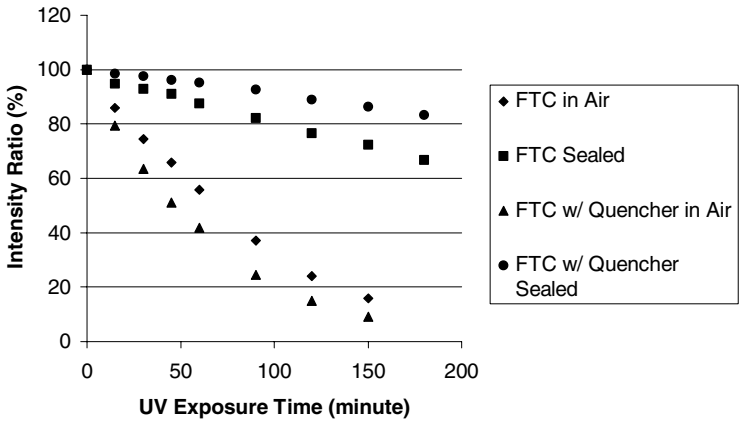

Figure 15. The photostability of FTC/PMMA materials with and without singlet oxygen scavengers is shown.

dependence of photodecomposition kinetics upon lattice hardness. Addition of singlet oxygen quenchers act to plasticize the polymer lattice, thus increasing oxygen diffusion rates and photochemical decomposition. Thus, under oxygen saturation where the scavenging effect of low concentrations of singlet oxygen quenchers is quickly lost but the effect of lattice plasticization persists, the most rapid photodegradation is observed. The role of secondary decomposition mechanisms remains less clear at this point. We have used high power pulse techniques capable of femtosecond time resolution to examine two-photon absorption [217] and have attempted, without success, to detect directly one- or two-photon decomposition mechanisms. The only mechanism that we are able to identify at present is the generation of singlet oxygen starting with chromophore interband electronic excitation.

Based on prototype device studies it would appear that packaged organic electro-optic devices could satisfy Telacordia standards with respect to photochemical stability: however, this has not been formally demonstrated to the present time. Clearly, the photochemical stability of active electro-optic materials is an issue that deserves more study, particularly under conditions more relevant to in-field operation at telecommunications wavelengths. The same applies to cladding materials and particularly to cladding materials hardened by UV irradiation. For example, no studies have been carried out on the effects of impurities on photochemical decomposition.

4. Auxiliary materials properties

Organic electro-optic thin film materials must exhibit a number of auxiliary properties including low optical loss. Optical loss involves loss from both absorption and scattering mechanisms. Measurement of optical loss by a variety of techniques ranging from photothermal deflection spectroscopy (PDS) to the Teng [218] immersion method have been discussed elsewhere [11, 26] and will not be reviewed here. Figure 14 illustrates data obtained by the method of Teng [218]. Absorption at telecommunications wavelengths arises from overtone vibrational absorptions associated with hydrogen or, more specifically, with OH, NH or CH groups. For a normal polymer material, such absorption contributes to optical loss ranging between 1 and 2 dB cm^{-1} at telecommunications wavelengths. Electro-optic chromophores have reduced proton (hydrogen) density due to unsaturation associated with the pi-electron structure. As is shown in figure 16, lower optical loss is often observed in a chromophore/polymer composite than in the pure polymer. Partial fluorination often leads to reduced optical loss (to values of the order of 0.5–0.9 dB cm^{-1}) and heavy fluorination (proton replacement) can lead to loss values as low as 0.1 dB cm^{-1} for electro-optic materials. Comparable values are typically obtained for passive fluorinated polymers. Scattering associated with processing can also contribute to optical loss and this contribution can be very high indeed when phase separation occurs. We shall discuss scattering losses again when we discuss fabrication of waveguide structures by reactive ion etching techniques. For the present, we note that phase separation associated with spin casting and electric field poling processes can lead to high scattering losses. With care, such losses can be kept to insignificant values (a few tenths of dB cm^{-1}). Deposition of cladding layers and electrodes can lead to scattering losses if pitting of the active polymer layer (e.g. by the spin casting solvent used to deposit the cladding layer) results. As might be expected, a hardened electro-optic material lattice is the answer to avoiding scattering loss associated with deposition of cladding layers and electrodes and reactive ion etching of buried channel waveguide structures.

Control of the index of refraction, dielectric permittivity and conductivity of core and cladding thin film layers is important for obvious reasons for the influence on optical mode confinement, radiofrequency power requirements and poling efficiency. For example, fluorination lowers the index of refraction, which can have consequences for mode confinement unless a compatible cladding material is utilized.

Great flexibility in modifying the molecular structure of organic materials is a significant advantage in optimizing both electro-optic and auxiliary properties of organic electro-optic materials. Optimum properties will vary from application to application and organic materials permit materials to be optimized for each specific device application. For example, organic electro-optic materials can be tailored to be compatible with a wide variety of substrate materials including flexible materials such as Mylar. This compatibility with diverse materials can be exploited in the development of highly integrated device structures.

5. Buried channel waveguide fabrication and integration

The basic fabrication of buried channel waveguides by reactive ion etching and photochemical methods has been reviewed elsewhere [18, 26] and will not be reviewed in depth here. As noted in these earlier reviews, very low optical loss values (excess loss values of 0.01 dB cm^{-1} [21, 22]) can be obtained providing appropriate processing conditions are maintained. For reactive ion etching this means maintaining the conditions of a ‘chemical’ etch (minimum kinetic energy for the reactive ions) to avoid pitting and thus loss associated with scattering from waveguide surface roughness. Lattice hardness also plays a role in minimizing

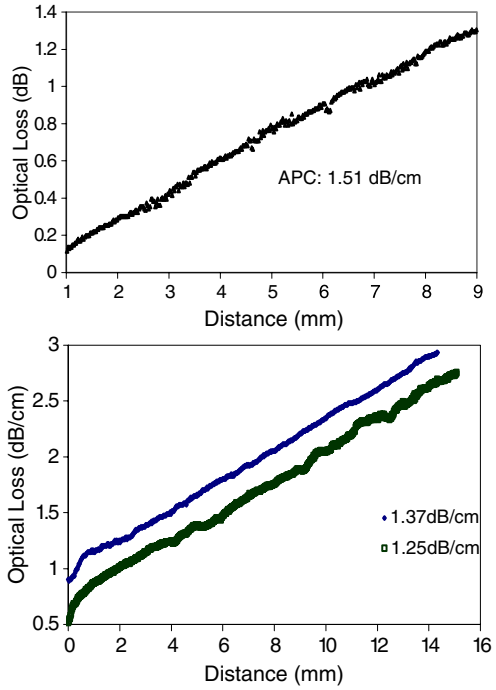

Figure 16. Optical loss for a film of pure APC polymer and for a 25 wt% chromophore/APC polymer composite are shown.

surface roughness, with harder materials yielding smoother surfaces. Photochemical processing has been shown to permit post-fabrication tuning of optical circuit elements such as power splitters and Mach–Zehnder interferometers [219–221].

Integration, including vertical integration, of electro-optic circuitry with VLSI electronic circuitry has been demonstrated and reviewed [26]. The key to vertical integration is the deposition of a planarizing polymer layer on top of the VLSI circuitry to take out the surface variations of the VLSI chip. The re-flow properties of planarizing polymers readily permit optical quality deposition surfaces to be obtained. Thin films of electro-optic materials are then deposited on the planarized polymer surfaces by spin casting. Normal electric field poling can be carried out provided proper grounding is used to protect the underlying semiconductor electronics. Interconnection between the electro-optic circuit electrodes and the semiconductor electronics requires the fabrication of deep vias through the planarizing polymer layer. This is accomplished by a combination of oxygen and CF_4 reactive ion etching and spin-on-glass technology.

Integration of electro-optic waveguide circuitry with silica fibre optics is a matter of addressing the mode mismatch that exists between these two types of transmission structures [11]. At telecommunications wavelengths, optical modes in silica fibres have a spherical shape with a diameter of approximately 10 μm. The optical modes in active electro-optic waveguides are ellipsoidal in shape with dimensions of approximately 1.5 $\times$ 5 μm. These dimensions are defined by the requirement of minimizing drive electrode spacing. Thus, a considerable mode size mismatch exists. This is in contrast to lithium niobate waveguides where the dominant problem in optical impedance matching relates to the index difference between waveguide materials. Several options exist for achieving effective coupling

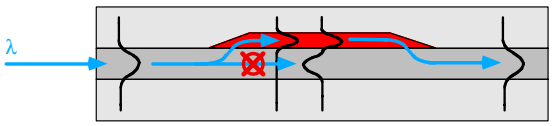

Figure 17. An in-line wedge electro-optic modulator structure is shown.

of light into and out of organic electro-optic waveguides. These include spherical lens, tapered transition structures [23] and in-line type wedge structures (see figure 17) based on the vertical slope fabrication used in producing three-dimensional optical circuits [25, 28]. With the latter two structures, the optical mode in one type of waveguide is progressively transformed into a mode supported by the second type of waveguide. Spherical or Luneburg type lenses act to focus light into the receiving waveguide. Tapered transition and in-line wedge type mode transformers are capable of reducing per facet coupling losses to a few tenths of a decibel. Total insertion loss is a combination of coupling loss and loss that occurs when the optical wave is propagating in the active electro-optic waveguide. If a 3 cm electro-optic waveguide is used with a waveguide propagation loss of 1 dB cm^{-1}, then realization of per facet coupling losses of less than 1 dB per transition permits total insertion losses of less than 5 dB to be obtained. Insertion loss values as low as 3 dB have been obtained for 2 cm device structures. For more in-depth reviews of optical impedance matching between silica fibre and organic electro-optic waveguides, the reader is referred to [11] and [26].

We have already referred to a critical advance in the fabrication of polymeric waveguide circuitry that has permitted both low insertion loss devices and three-dimensional circuitry to be produced [11, 25, 28]. This advance involved the ability to fabricate a vertical slope using grey-scale mask, shadow mask or off-set reactive ion etching methods. Once a vertical slope is produced, spin casting permits the realization of a material transition that preserves the vertical slope. More recently this type of processing has been used to fabricate add/drop wavelength filters, 3D routers and active WDM systems based on ring microresonators [36, 37].

6. Devices

The relationship of V_{pi} to device parameters has been discussed elsewhere for Mach–Zehnder interferometers, birefringent modulators and directional couplers [57]. Different device structures can have different dependences on the non-zero electro-optic tensor components r_{33} and r_{13} (where $r_{33} = 3r_{13}$) for poled organic materials. For example, V_{pi} for birefringent modulators depend on the difference between coefficients $(r_{33} - r_{13})$ while V_{pi} for Mach–Zehnder and directional coupler devices depend only on r_{33} [57]. Similar discussions can be found for push–pull Mach–Zehnder devices [42, 43], cascaded prism spatial light modulators [38–40] and ring microresonators [36, 37]. For electro-optic materials, device parameters are defined by a variety of variables including electro-optic coefficients, material optical loss, material index of refraction and material dielectric constant. The relatively modest electro-optic coefficients that have been available at the present time have necessitated long interactions lengths, e.g. of the order of 1–3 cm (V_{pi} is inversely proportional to the interaction length). The spacing of drive electrodes (V_{pi} is linearly dependent on electrode spacing) is defined by the need to incorporate cladding layers to prevent the propagating optical field from sensing metal electrodes. Optical wave–electrode interaction would result in unacceptably high optical loss. For typical devices, this results in an electrode separation of about 8–12 μm. However, such separation may be reduced by use of photonic bandgap waveguide structures

to achieve tighter confinement of light. Such structures are also useful in minimizing bending losses and indeed light can be propagated around right angle bends with such structures.

Electro-optic devices can be divided into three fundamental types: stripline devices, prism devices and microresonator devices. All three types can be engineered to permit long interaction lengths to be realized but with different consequences for bandwidth, drive voltage, device size and device function. The interaction length in stripline devices is determined by the length of the stripline electrodes while the interaction length in cascaded prism devices is determined by the base length of the cascaded prism structure [11, 38–40, 42, 43]. The interaction length has a small effect on bandwidth for stripline and cascaded prism devices and directly affects the size of the device. The situation is quite different for ring microresonators. As devices based on stripline and cascaded prism structures have been reviewed and discussed elsewhere [11, 38–40, 42, 43] we limit our remarks to the brief comments already made. The rest of our discussion of devices is devoted to recently studied ring microresonator devices [36, 37]. Ring microresonators involve whispering gallery modes. For light to be coupled into ring microresonators, two conditions must be satisfied:

(1) the circumference of the ring must be a multiple of the wavelength of the resonant light (this results in wavelength selectivity), and
(2) the velocity of light in the ring much match the velocity of input light (electro-optic tuning of the index of refraction of the ring permits this second condition to be satisfied with voltage control).

We have also recently begun to explore ring microresonator structures, including double ring structures, that can be employed not only as electrical-to-optical signal transducers but also as wavelength-selective filters and optical signal routers [36, 37]. Both single-ring resonators (such as shown in figure 18) and double-ring (exploiting the Vernier effect) devices have been fabricated. Single-ring resonators can be exploited for active wavelength division multiplexing (WDM–such as shown in figure 19), wavelength-selective filters, optical routers and tunable laser applications. Double-ring resonators can be used to fabricate fast, voltage-tunable light sources for optical frequency shift keying and, eventually, optical CDMA systems.

The fabrication of the active ring microresonator structure shown in figure 18 starts with a gold-coated silicon substrate. A lower cladding (UV-15 or ZPU13) is spin-coated onto the device [36, 37]. Next, the electro-optic material (in the present case, a CLD/APC polymer composite material) is spin-coated and corona poled. The electro-optic material is patterned using optical lithography and the ring waveguide is etched using reactive ion etching. A middle cladding layer is then spin-coated, the trenches are formed and the waveguide layer is spin-coated. Finally, the upper cladding layer is made and the upper electrode deposited.

Standard commercial software (such as TempSelene) has been used to design device structures. The dimensions of the ring microresonators (and thus critical performance parameters such as quality factor (Q), free spectral range (FSR) and finesse) are determined by the differences in the index of refraction of the core and cladding polymeric materials. Since index of refraction differences are quite small ($\Delta n = 0.1$–0.3) in the work described here, ring resonator radii are limited to 250–25 μm. Bending loss, scattering loss and material loss are the main optical loss mechanisms for ring microresonators. Bending loss is primarily determined by the index difference between the core and the cladding and thus sets the minimum diameter (and FSR) for a ring resonator. The dimensions just cited correspond to a bending loss of 1 dB cm^{-1}. Material loss is typically of the order of 1 dB cm^{-1}. Scattering loss arises from the rough surface of the waveguide (defined by the quality of the optical mask used to define the ring microresonator). For the range of ring microresonators considered here (typical surface roughness is of the order of 20 nm), scattering loss values can range between

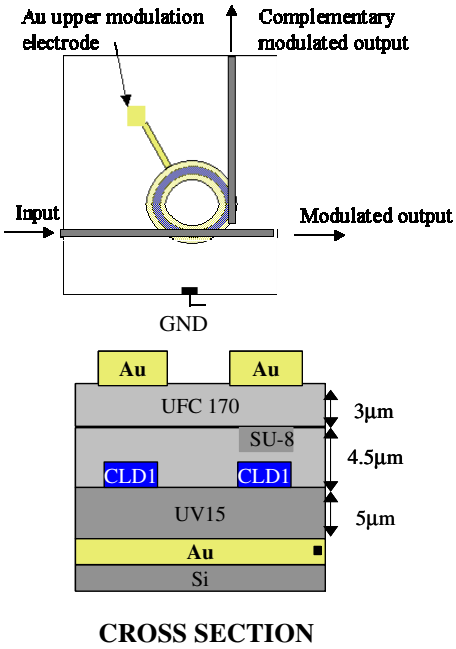

Figure 18. The top (upper) and cross-sectional (lower) views of an electro-optic ring microresonator are shown.

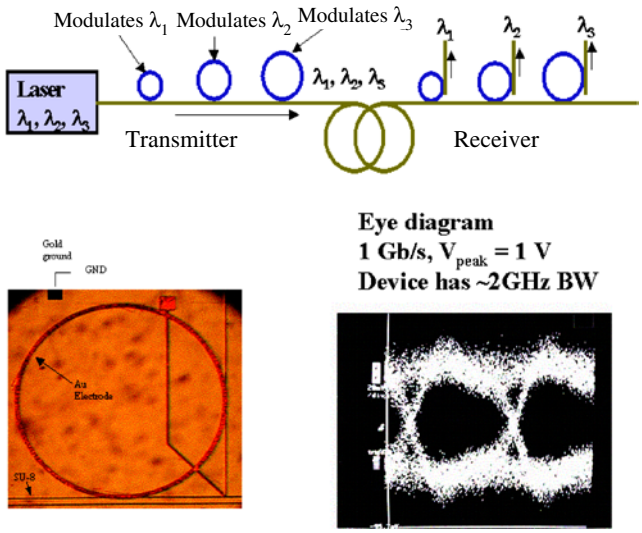

Figure 19. The schematic of an active WDM transmitter receiver based on electro-optic ring microresonators is shown (upper). A micrograph of a single-ring microresonator is shown in the lower left and the eye diagram for operation of one wavelength channel is shown in the lower right.

2 and 20 dB cm^{-1} and are certainly the dominant loss mechanism. Q values of the order of 100 000 are easily obtained for the materials used in this study. Microresonators have been fabricated for operation at both the 1.3 and 1.5 μm telecommunications bands. Wavelength-

selective filters with finesse as high as 141 have been achieved. FSR values of 5 and 8 nm were observed at 1.3 and 1.55 μm, respectively. The sensitivity–bandwidth product (BW/V_{FWHM}) is given by $K\nu n^3 r_{33}/2n_e d$, where K is the confinement factor, n is the refractive index of the electro-optic material, n_e is the effective index of the microring, ν is the optical frequency, r_{33} is the electro-optic coefficient and d is the electrode spacing. With current materials and device structures, values between 2 and 10 GHz V^{-1} are obtained. It is interesting to note that, if the best currently obtainable 10 Gb s^{-1} per wavelength data rate is extended to 50 wavelengths, then a modulation rate of 500 Gb s^{-1} would be possible.

We have also examined double-ring microresonators. The wavelength of maximum transmission from input to output occurs when both microrings are resonant. Since the rings have different diameters, the mode spacing is different and the wavelength of maximum transmission changes by a large amount as the resonant wavelength of one of the rings is tuned. There is a Vernier effect and the tuning is discrete. If the wavelength of one of the rings is tuned by $\Delta\lambda$, the wavelength of the maximum transmission tunes by $M\Delta\lambda$ where $M = d_1/(d_1 - d_2)$ and d_1 and d_2 are the diameters of the two microrings. Fabricating microrings with diameters of 240 and 246 μm, we have realized $M = 40$. We have demonstrated both voltage (electro-optic) and thermal tuning of polymeric double microrings and demonstrated tuning of an oscillator across the band of the erbium amplifier (1520–1560 nm). A voltage tuning of 0.04 nm V^{-1} and thermal tuning of 0.6 nm mW^{-1} was observed. Side mode suppression was greater than 30 dB. A distinct advantage of polymeric ring microresonators is that both thermal and athermal designs can be implemented. The changes of the index of refraction with temperature can be used to cancel the change associated with thermal expansion leading to temperature-independent device operation. It is interesting to note that photochemical instability has not been observed to be a problem with microresonator structures fabricated at present.

7. Summary and future prognosis

Theory has permitted the realization of materials with electro-optic coefficients approximately four times greater than lithium niobate. Moreover, theory strongly suggests that electro-optic activity can be further increased to an order of magnitude greater than lithium niobate (i.e. to approximately 300 pm V^{-1}). To obtain electro-optic coefficients greater than 1000 pm V^{-1} will require the use of additional ordering forces such as ionic or hydrogen bonding forces to achieve noncentrosymmetric crystals of organic chromophores. Conceivably theory could guide the preparation of such crystals. The electro-optic activity of currently available materials is attracting considerable industrial attention and novel prototype devices are being developed. For example, new concepts in electrical/optical signal control are being explored in a new National Science Foundation Science and Technology Center on Materials and Devices for Information Technology Research [222]. Professor A Yariv (Cal Tech) is exploring the use of voltage control of critical coupling to microresonator structures for optical switching while Professor A Scherer (Cal Tech) is exploring photonic bandgap structures. This latter class of materials could conceivably lead to a new family of high sensitivity sensors. A wide range of other device applications utilizing organic electro-optic materials, ranging from optical gyroscopes to phased array radar systems [11], are under investigation in federal and industrial research laboratories. In addition to improving electro-optic activity, the exceptional bandwidth and processing capabilities are strong drivers for such exploration. The major issues determining short-term application of organic electro-optic materials are likely those of thermal and photochemical stability. Organic materials and photonic technology definitely afford weight advantages for space applications where launch weight translates into cost. Also,

organic electro-optic materials appear to be particularly immune to damage from high-energy irradiation. Clearly, organic electro-optic materials have the potential for impacting a variety of applications in the defense, computing and telecommunications industries.

Acknowledgments

The author would like to thank the National Science Foundation (grants DMR-0092380, DMR-0103009, and DMR-0120967) for partial support of this research and his many faculty colleagues, graduate students, postdoctoral research associates and undergraduate research assistants for invaluable assistance. The opinions expressed in this article are those of the author and not necessarily those of his colleagues nor the National Science Foundation.

References

[1] Zyss J and Ledoux I 1994 *Chem. Rev.* **94** 77
[2] Andraud C, Zabulon T, Collet A and Zyss J 1999 *Chem. Phys.* **245** 243
[3] Lee M, Katz H E, Erben C, Gill D M, Gopalan P, Heber J D and McGee D J 2002 *Science* **298** 1404
[4] Chen D, Fetterman H R, Chen A, Steier W H, Dalton L R, Wang W and Shi Y 1997 *Proc. SPIE* **3006** 314
[5] Chen D, Fetterman H R, Chen A, Steier W H, Dalton L R, Wang W and Shi Y 1997 *Appl. Phys. Lett.* **70** 3335
[6] Fetterman H, Udupa A, Bhattacharya D, Erlig H, Ali M, Chang Y and Dalton L R 1998 *Terahertz Electronic Proc.* p 102
[7] Hayden M 2003 private communication of unpublished results on terahertz signal generation and detection using organic electro-optic materials
[8] Chen D, Bhattacharya D, Udupa A, Tsap B, Fetterman H R, Chen A, Lee S S, Chen J, Steier W H and Dalton L R 1999 *IEEE Photonics Technol. Lett.* **11** 54
[9] Bechtel J H, Shi Y, Zhang H, Steier W H, Zhang C H and Dalton L R 2000 *Proc. SPIE* **4114** 58
[10] Becker M W, Sapochak L S, Dalton L R, Shi Y, Steier W H and Jen A K 1994 *Chem. Mater.* **6** 104
[11] Dalton L R 2002 *Adv. Polym. Sci.* **158** 1
[12] Wise D L, Wnek G, Trantolo D J, Cooper T M and Gresser J D (ed) 1998 *Electrical and Optical Polymer Systems* (New York: Dekker)
[13] Hornak L A (ed) 1992 *Polymers for Lightwave and Integrated Optics* (New York: Dekker)
[14] Nalwa H S and Miyata S (ed) 1997 *Nonlinear Optics of Organic Molecules and Polymers* (Boca Raton, FL: Chemical Rubber Company Press)
[15] Lindsay G A and Singer K D (ed) 1995 *Polymers for Second-Order Nonlinear Optics* (Washington, DC: American Chemical Society)
[16] Evmenenko G, van der Boom M E, Kmetko J, Dugan S W, Marks T J and Dutta P 2001 *J. Chem. Phys.* **115** 6722
[17] Zhao Y G, Wu A, Lu H L, Chang S, Lu W K, Ho S T, van der Boom M E and Marks T J 2001 *Appl. Phys. Lett* **79** 587
[18] Dalton L R, Harper A W, Ghosn R, Steier W H, Ziari M, Fetterman H, Shi Y, Mustacich R, Jen A K Y and Shea K J 1995 *Chem. Mater.* **7** 1060 and references contained therein
[19] Kalluri S, Chen A, Chuyanov V, Ziari M, Steier W H and Dalton L R 1995 *Proc. SPIE* **2527** 375
[20] Kalluri S, Ziari M, Chen A, Chuyanov V, Steier W H, Chen D, Jalali B, Fetterman H R and Dalton L R 1996 *IEEE Photonics Technol. Lett.* **8** 644
[21] Steier W H, Kalluri S, Chen A, Garner S, Chuyanov V, Ziari M, Shi Y, Fetterman H, Jalali B, Wang W, Chen D and Dalton L R 1996 *Mater. Res. Soc. Symp. Proc.* **413** 147
[22] Chen A, Kaviani K, Remple A, Kalluri S, Steier W H, Shi Y, Liang Z and Dalton L R 1996 *J. Electrochem. Soc.* **143** 3648
[23] Chen A, Chuyanov V, Marti-Carrera F I, Garner S, Steier W H, Chen J, Sun S and Dalton L R 1997 *Proc. SPIE* **3005** 65
[24] Garner S, Chuyanov V, Chen A, Lee S S, Steier W H and Dalton L R 1998 *Proc. SPIE* **3278** 259
[25] Garner S M, Lee S S, Chuyanov V, Yacoubian A, Chen A, Steier W H, Zhu J, Chen J, Wang F, Ren A S and Dalton L R 1998 *Proc. SPIE* **3491** 421
[26] Dalton L R, Harper A W, Ren A, Wang F, Todorova G, Chen J, Zhang C and Lee M 1999 *Ind. Eng. Chem. Res.* **38** 8
[27] Garner S M, Chuyanov V, Lee S S, Chen A, Steier W H and Dalton L R 1999 *IEEE Photonics Technol. Lett.* **11** 842

[28] Garner S M, Lee S S, Chuyanov V, Chen A, Yacoubian A, Steier W H and Dalton L R 1999 *IEEE J. Quantum Electron.* **35** 1146
[29] Steier W H, Chen A, Lee S S, Garner S, Zhang H, Chuyanov V, Dalton L R, Wang F, Ren A S, Zhang C, Todorova G, Harper A W, Fetterman H R, Chen D, Udupa A, Bhattacharya D and Tsap B 1999 *Chem.Phys.* **245** 487
[30] Chen A, Chuyanov V, Marti-Carrera F I, Garner S M, Steier W H, Chen J, Sun S S and Dalton L R 2000 *Opt. Eng.* **39** 1507
[31] Lee S S, Garner S M, Chuyanov V, Zhang H, Steier W H, Wang F, Dalton L R, Udupa A H and Fetterman H R 2000 *IEEE J. Quantum Electron.* **36** 527
[32] Oh M C, Zhang H, Szep A, Chuyanov V, Steier W H, Zhang C, Dalton L R, Erlig H, Tsap B and Fetterman H R *Appl. Phys. Lett.* **76** 3525
[33] Zhang H, Oh M C, Szep A, Steier W H, Zhang C, Dalton L R, Erlig H, Chang D H and Fetterman H R 2001 *Appl. Phys. Lett.* **78** 3136
[34] Zhang C, Dalton L R, Oh M C, Zhang H and Steier W H 2001 *Chem. Mater.* **13** 3043
[35] Oh M C, Zhang H, Zhang C, Erlig H, Chang Y, Tsap B, Chang D, Szep A, Steier W H, Fetterman H R and Dalton L R 2001 *J. Sel. Top. Quantum Electron.* **7** 826
[36] Rabiei P, Steier W H, Zhang C and Dalton L R 2002 *J. Lightwave Technol.* **20** 1968
[37] Rabiei P, Steier W H, Zhang C and Dalton L R 2002 *Int. Opt. Commun.* 14
[38] Sun L, Kim J H, Jang C H, Maki J J, An D, Zhou Q, Lu X, Taboada J M, Chen R T, Tang S, Zhang H, Steier W H, Ren A S and Dalton L R 2000 *Proc. SPIE* **3950** 98
[39] Sun L, Kim J, Jang C, An D, Lu X, Zhou Q, Taboada J M, Chen R T, Maki J J, Tang S, Zhang H, Steier W H, Zhang C and Dalton L R 2001 *Opt. Eng.* **40** 1217
[40] Kim J H, Sun L, Jang C H, An D, Taboada J M, Zhou Q, Lu X, Chen R T, Han X, Tang S, Zhang H, Steier W H, Ren A and Dalton L R 2001 *Proc. SPIE* **4279** 37
[41] An D, Shi Z, Sun L, Taboada J M, Zhou Q, Lu X, Chen R T, Tang S, Zhang H, Steier W H, Ren A and Dalton L R 2000 *Appl. Phys. Lett.* **76** 1972
[42] Shi Y, Zhang C, Zhang H, Bechtel J H, Dalton L R, Robinson B H and Steier W H 2000 *Science* **288** 119
[43] Shi Y, Lin W, Olson D J, Bechtel J H, Zhang H, Steier W H, Zhang C and Dalton L R 2000 *Appl. Phys. Lett.* **77** 1
[44] Ermer S P, Girton D G, Dries L J, Taylor R E, Eades W D, Van Eck T E, Moss A S and Anderson W W 2000 *Proc. SPIE* **3949** 148
[45] Yacoubian A, Chuyanov V, Garner S M, Steier W H, Ren A S and Dalton L R 2000 *IEEE J. Sel. Top. Quantum Electron.* **6** 810
[46] Lee S S, Udupa A H, Erlig H, Zhang H, Chang Y, Zhang C, Chang D H, Bhattacharya D, Tsap B, Steier W H, Dalton L R and Fetterman H R 1999 *IEEE Microw. Guid. Wave Lett.* **9** 357
[47] Chang D H, Erlig H, Oh M C, Zhang C, Steier W H, Dalton L R and Fetterman H R 2000 *IEEE Photonics Technol. Lett.* **12** 537
[48] Fetterman H R, Chang D H, Erlig H, Oh M, Zhang C H, Steier W H and Dalton L R 2000 *Proc. SPIE* **4114** 44
[49] Prasad P N and Williams D J 1991 *Introduction to Nonlinear Optical Effects in Molecules and Polymers* (New York: Wiley)
[50] Williams D J (ed) 1993 *Nonlinear Optical Properties of Organic Polymeric Materials* (Washington, DC: American Chemical Society)
[51] Zyss J (ed) 1994 *Molecular Nonlinear Optics* (New York: Academic)
[52] Burland D M, Miller R D and Walsh C A 1994 *Chem. Rev.* **94** 31
[53] Kanis D R, Ratner M A and Marks T J 1994 *Chem. Rev.* **94** 195
[54] Nie W 1993 *Adv. Mater.* **5** 520
[55] Marks T J and Ratner M A 1995 *Angew. Chem. Int. Ed. Engl.* **34** 155
[56] Bosshard C, Sutter K, Pretre P, Hulliger J, Florsheimer M, Kaatz P and Gunter P 1995 *Organic Nonlinear Optical Materials* (New York: Gordon and Breach)
[57] Dalton L R, Harper A W, Wu B, Ghosn R, Laquindanum J, Liang Z, Hubbel A and Xu C 1995 *Adv. Mater.* **7** 519
[58] Sun S S, Maaref S, Alam E, Wang Y, Fan Z, Bahoura M, Higgins P T and Bonner C E Jr 2001 *Proc. SPIE* **4580** 297
[59] Cooper K L, Claus R O, Mecham J B, Huie K and Swavey R 2001 *Proc. SPIE* **4512** 93
[60] Dumont M L 2001 *Proc. SPIE* **4461** 149
[61] Zadrozna I and Myslek M 2001 *J. Appl. Polym. Sci.* **80** 1374
[62] Marder S R, Kippelen B, Jen A K Y and Peyghammbarian N 1997 *Nature* **388** 845
[63] Brasselet S and Zyss J 1998 *Proc. SPIE* **3469** 154

[64] Dalton L R and Bale D H 2003 Nonlinear optical materials *Kirk-Othmer Encyclopedia of Chemical Technology* 5th edn (New York: Wiley)
[65] Katz H E, Singer K D, Sohn J E, Dirk C W, King L A and Gordon H M 1987 *J. Am. Chem. Soc.* **109** 6561
[66] Cheng L T, Tam W, Marder S R, Stiegman A E, Rikken G and Spangler C W 1991 *J. Phys. Chem.* **95** 10643
[67] Rao V P 1992 *Proc. SPIE* **1775** 32
[68] Dirk C W 1990 *Chem. Mater.* **2** 700
[69] Marder S R, Cheng L T, Tiemann B G, Friedli A C, Blanchard-Desce M, Perry J W and Skindhøj J 1994 *Science* **263** 511
[70] Jen A K Y, Wong K Y, Rao V P, Drost K, Caldwell B and Mininni R 1994 *Mater. Res. Soc. Symp. Proc.* **328** 413
[71] Wang C H, Woodford J N, Zhang C and Dalton L R 2001 *J. Appl. Phys.* **89** 4209
[72] Lalama S J and Garito A F 1979 *Phys. Rev.* A **20** 1179
[73] Oudar J L and Chemla D S 1977 *J. Chem. Phys.* **66** 2664
[74] Ward J 1965 *Rev. Mod. Phys.* **37** 1
[75] Orr J B and Ward J F 1971 *Mol. Phys.* **20** 513
[76] Oudar J L 1977 *Chem. Phys.* **67** 446
[77] Heflin J R, Wong K Y, Zamani-Khamiri O and Garito A F 1988 *Phys. Rev.* B **38** 1573
[78] Garito A F, Wong K Y, Cai Y M, Man H T and Zamani-Khamiri O 1986 *Proc. SPIE* **682** 2
[79] Bredas J L, Adant C, Tackx P, Persoons A and Pierce B M 1994 *Chem. Rev.* **94** 243
[80] Champagne B and Kirtman B 1999 *Chem. Phys.* **245** 211
[81] Lipinski J and Bartkowiak W 1999 *Chem. Phys.* **245** 263
[82] Painelli A 1999 *Chem. Phys.* **245** 185
[83] Kanis D R, Ratner M A and Marks T J 1994 *Chem. Rev.* **94** 195
[84] Di Bello S, Fragala I, Ratner M A and Marks T J 1995 *Chem. Mater.* **7** 400
[85] Albert I D L, Marks T J and Ratner M A 1996 *J. Phys. Chem.* **100** 9714
[86] Marder S R, Beratan D N and Cheng L T 1991 *Science* **252** 103
[87] Gorman C B and Marder S R 1993 *Proc. Natl Acad. Sci. USA* **90** 11297
[88] Marder S R and Perry J W 1994 *Science* **263** 1706
[89] Bourhill G, Cheng L T, Lee G, Marder S R, Perry J W, Perry M J and Tiemann B G 1994 *Mater. Res. Soc. Symp. Proc.* **328** 625
[90] Marder S R, Gorman C B, Meyers F, Perry J W, Bourhill G, Bredas J L and Pierce B M 1994 *Science* **265** 632
[91] Jen A K Y, Cai Y, Bedworth P V and Marder S R 1997 *Adv. Mater.* **9** 132
[92] Pierce B M, Zyss J and Joffre M 1993 *Proc. SPIE* **2025** 3
[93] Alain V, Redoglia S, Blanchard-Desce M, Lebus S, Lukaszuk K, Wortmann R, Gubler U, Bosshard C and Gunter P 1999 *Chem. Phys.* **245** 51
[94] Balakina M Y, Li J, Geskin V M, Marder S R and Bredas J L 2000 *J. Chem. Phys.* **113** 9598
[95] Lacroix P G, Malfant I, Iftime G, Razus A C, Nakatani K and Delaire J A 2000 *Chem. Eur. J.* **6** 2599
[96] Sahraoui B, Kityk I V, Ledoux-Rak I N, Nguyen T T A, Salle M and Gorgues A 2000 *Proc. SPIE* **4089** 876
[97] Szymusiak H, Zielinski R, Dormagalska B W and Wilk K A 2000 *Comput. Chem.* **24** 369
[98] Breitung E M, Shu C F and McMahon R J 2000 *J. Am. Chem. Soc.* **122** 1154
[99] Zamani-Khamiri O, Panakal A, Cai Y M and Garito A F 1998 *Proc. SPIE* **3474** 2
[100] Barlow S, Bunting H E, Ringham C, Green J C, Bublitz G U, Boxer S G, Perry J W and Marder S R 1999 *J. Am. Chem. Soc.* **121** 3715
[101] Base K, Tierney M T, Fort A, Muller J and Grinstaff M W 1999 *Inorg. Chem.* **38** 287
[102] Blanchard-Desce M, Alain V, Bedworth P V, Marder S R, Fort A, Runser C, Barzoukas M, Lebus S and Wortmann R 1997 *Chem. Eur. J.* **3** 1091
[103] Albert I D L, Marks T J and Ratner M A 1997 *J. Am. Chem. Soc.* **119** 6575
[104] Albert I D L, Marks T J and Ratner M A 1997 *J. Am. Chem. Soc.* **119** 3155
[105] Di Bella S, Lanza G, Fragala I, Yitzchaik S, Ratner M A and Marks T J 1997 *J. Am. Chem. Soc.* **119** 3003
[106] Diaz J L, Villacampa B, Lopez-Calahorra F and Velasco D 2002 *Chem. Mater.* **14** 2240
[107] Castaldo A, Centroe R, Peluso A, Sirigu A and Tuzi A 2002 *Struct. Chem.* **13** 27
[108] Moran A M, Egolf D S, Blanchard-Desce M and Kelley A M 2002 *J. Chem. Phys.* **116** 2542
[109] Moore A J, Chesney A, Bryce M R, Batsanov A S, Kelly J F, Howard J A K, Perepichka I F, Perepichka D F, Meshulam G, Berkovic G, Kotler Z, Mazor R and Khodorkovsky V 2001 *Eur. J. Org. Chem.* **14** 2671
[110] Parusel A B J, Schamschule R and Kohler G 2001 *J. Mol. Struct. (Theochem)* **544** 253
[111] Hernandez V, Casado J, Higuchi H and Lopez N J T 2001 *Synth. Met.* **119** 553
[112] Xiang L, Liu Y G, Jiang A G and Huang D Y 2001 *Chem. Phys. Lett.* **338** 167
[113] Prezhdo O V 2002 *Adv. Mater.* **14** 597

[114] Yamada S, Cai Y M, Shi R F, Wu M H, Chen W D, Qian Q M and Garito A F 1994 *Mater. Res. Soc. Symp. Proc.* **328** 523
[115] He M, Leslie T M and Sinicropi J A 2002 *Chem. Mater.* **14** 4662
[116] He M, Leslie T M, Sinicropi J A, Garner S M and Reed L D 2002 *Chem. Mater.* **14** 4669
[117] Jean-Luc Bredas 2003 private communication of unpublished results
[118] Katti K V, Raghuraman K, Pillarsetty N, Karra S R, Gulotty R J, Chartier M A and Langhoff C A 2002 *Chem. Mater.* **14** 2436
[119] Kim O K, Fort A, Barzoukas M, Blanchard-Desce M and Lehn J M 1999 *J. Mater. Chem.* **9** 2227
[120] Ermer S, Lovejoy S, Leung D S, Warren H, Moylan C R and Twieg R J 1998 *Mater. Res. Soc. Symp. Proc.* **488** 243
[121] Wu X, Wu J, Liu Y and Jen A K Y 1999 *Chem. Commun.* 2391
[122] Cai C, Liakatas K, Wong M S, Boesch M, Bosshard C, Gunter P, Concilio S, Tirelli N and Suter U W 1999 *Org. Lett.* **1** 1847
[123] Jen A K Y, Liu Y, Zheng L, Liu S, Drost K J, Zhang Y and Dalton L R 1999 *Adv. Mater.* **11** 452
[124] Park K H, Lim J T, Song S, Lee Y S, Lee C J and Kim N 1999 *React. Funct. Polym.* **40** 117
[125] Garin J, Oruna J, Ruperez J I, Alcala R, Villacampa B, Sanchez C, Martin N, Segura J L and Gonzalez M 1998 *Tetrahedron Lett.* **39** 3577
[126] Shu C F and Wang Y K 1998 *J. Mater. Chem.* **8** 833
[127] Belfield K D, Chinna C and Schafer K J 1997 *Tetrahedron Lett.* **38** 6131
[128] He M, Leslie T M and Sinicropi J A 2002 *Chem. Mater.* **14** 2393
[129] Hua J, Luo J, Qin J, Shen Y, Zhang Y and Lu Z 2002 *J. Mater. Chem.* **12** 863
[130] Hua J, Zhang W, Li Z, Qin J, Shen Y, Zhang Y and Lu Z 2002 *Chem. Lett.* **2** 232
[131] Chen Y and Huang C F 2002 *Synth. Met.* **125** 387
[132] Zhang C, Dalton L R, Oh M C, Zhang H and Steier W H 2001 *Chem. Mater.* **13** 3043
[133] Perepichka D F, Perepichka I F, Bryce M R, Sokolov N I and Moore A J 2001 *J. Mater. Chem.* **11** 1772
[134] Moreno-Manas M, Pleixats R, Andreu R, Garin J, Orduna J, Vilacampa B, Levillain E and Salle M 2001 *J. Mater. Chem.* **11** 374
[135] Luo J, Hua J, Qin J, Cheng J, Shen Y, Lu Z, Wang P and Ye C 2001 *Chem. Commun.* **2** 171
[136] Wang C and Dalton L R 2000 *Tetrahedron Lett.* **41** 617
[137] Zhang C, Harper A W, Spells D S and Dalton L R 2000 *Synth. Commun.* **30** 1359
[138] Zhang C, Harper A W and Dalton L R 2001 *Synth. Commun.* **31** 1361
[139] Sun S S, Zhang C, Yang Z, Dalton L R, Garner S M, Chen A and Steier W H 1998 *Polymer* **39** 4977
[140] Wang F, Harper A W, He M, Ren A, Dalton L R, Garner S M, Yacoubian A, Chen A and Steier W H 1998 *Organic Thin Films ACS Symp. Series 695* (Washington, DC: American Chemical Society) p 252
[141] Chen J, Zhu J, Todorova G, He H, Dalton L R, Garner S, Chen A and Steier W H 1998 *Mater. Res. Soc. Symp. Proc.* **488** 151
[142] Jen A K Y, Liu Y, Zheng L, Liu S, Drost K J, Zhang Y and Dalton L R 1999 *Adv. Mater.* **11** 452
[143] Zhang C, Ren A S, Wang F, Zhu J, Dalton L R, Woodford J N and Wang C H 1999 *Chem. Mater.* **11** 1966
[144] Wang F, Harper A W, Lee M S, Dalton L R, Zhang H, Chen A, Steier W H and Marder S R 1999 *Chem. Mater.* **11** 2285
[145] Harper A W, Mao S S H, Ra Y S, Zhang C, Zhu J, Dalton L R, Garner S, Chen A and Steier W H 1999 *Chem. Mater.* **11** 2886
[146] Huang D, Zhang C, Dalton L R and Weber W P 2000 *J. Polym. Sci.* A **38** 546
[147] Liakatas I, Cai C, Bosch M, Jager M, Bosshard Ch, Gunter P, Zhang C and Dalton L R 2000 *Appl. Phys. Lett.* **76** 1368
[148] Pan J, Chen M, Warner W, He M, Dalton L and Hogen-Esch T 2000 *Macromolecules* **33** 4673
[149] Pan J, Chen M, Warner W, He M, Dalton L and Hogen-Esch T 2000 *Macromolecules* **33** 7835
[150] Huang D, Zhang C, Dalton L R and Weber W P 2000 *Des. Monomers Polym.* **3** 95
[151] Ma M, Chen B, Takafumi S, Dalton L R and Jen A K Y 2001 *J. Am. Chem. Soc* **123** 986
[152] Liu S, Haller M A, Ma H, Dalton L R, Jang S H and Jen A K Y 2003 Focused microwave-assisted synthesis of 2, 5-dihydrofuran derivatives as electron acceptors for highly efficient nonlinear optical chromophores *Adv. Mater.* **15** 603
[153] Jen A K Y, Luo J, Ma H, Liu S, Liu L, Haller M, Sassa T, Kang S H and Dalton L R 2002 *Proc. SPIE* **4798** 21
[154] Dalton L R, Robinson B H, Nielsen R, Jen A K Y and Steier W H 2002 *Proc. SPIE* **4798** 1
[155] Ma H, Liu S, Luo J, Suresh S, Liu L, Kang S H, Haller M, Sassa T, Jen A K Y and Dalton L R 2002 *Adv. Funct. Mater.* **12** 565
[156] Jen A K Y, Ma H, Sassa T, Liu S, Suresh S, Dalton L R and Haller M 2001 *Proc. SPIE* **4461** 172

[157] Jen A K Y, Luo J, Liu S, Haller M, Ma H, Liu L and Dalton L R 2003 Nanoscale tailoring of dendrimers and polymers for electro-optic devices *Proc. SPIE* **4991** at press
[158] Perry J W, Marder S R, Perry K J, Sleva E T, Yakymshyn C, Steward K R and Boden E P 1991 *Proc. SPIE* **1560** 302
[159] Steward K R 1994 *Photonics Spectra* **28** 104
[160] Thakur M, Su J, Bhowmik A and Zhou L 1999 *Appl. Phys. Lett.* **74** 635
[161] Pan F, McCallion K and Chiapetta M 1999 *Appl. Phys. Lett.* **74** 492
[162] Pan F, Wong M S, Bosshard C and Gunter P 1996 *Adv. Mater.* **8** 592
[163] Liakatas I, Wong M S, Bosshard C, Ehrensperger M and Gunter P 1997 *Ferroelectrics* **202** 299
[164] Meier U, Bosch M, Bosshard C, Pan F and Gunter P 1998 *J. Appl. Phys.* **83** 3486
[165] Sohma S, Takahashi H, Taniuchi T and Ito H 1999 *Chem. Phys.* **245** 539
[166] Kim W K and Hayden L M 1999 *J. Chem. Phys.* **111** 5212
[167] Dalton L R, Harper A W and Robinson B H 1997 *Proc. Natl Acad. Sci. USA* **94** 4842
[168] Dalton L R, Harper A W, Chen J, Sun S, Mao S S, Garner S, Chen A and Steier W H 1997 *Proc. SPIE* **CR68** 313
[169] Harper A W, Sun S, Dalton L R, Garner S M, Chen A, Kalluri S, Steier W H and Robinson B H 1998 *J. Opt. Soc. Am.* B **15** 329
[170] Robinson B H and Dalton L R 2000 *J. Phys. Chem.* **104** 4785
[171] Dalton L R, Robinson B H, Nielsen R, Jen A K Y and Steier W H 2002 *Proc. SPIE* **4798** 1
[172] Dalton L R, Robinson B H, Jen A K Y, Steier W H and Neilsen R 2003 *Opt. Mater.* **21** 19
[173] Piekara A 1938 *Z. Phys.* **108** 396
[174] Piekara A 1939 *Proc. R. Soc.* A **172** 360
[175] Luo J, Ma H, Haller M, Jen A K Y and Barto R R 2002 *Chem. Commun.* 888
[176] Luo J, Liu S, Haller M, Liu L, Ma H and Jen A K Y 2002 *Adv. Mater.* **14** 1763
[177] Percec V, Cho W D, Mosier P E, Ungar G and Yardley D J P 1998 *J. Am. Chem. Soc.* **120** 11061
[178] Hudson S D, Jung H T, Percec V, Cho W D, Johansson G, Ungar G and Balagurusamy V. S. K 1997 *Science* **278** 449
[179] Percec V, Schlueter D, Ungar G, Cheng S Z D and Zhang A 1998 *Macromolecules* **31** 1745
[180] Yacoubian A 1999 *PhD Thesis* University of Southern California, Los Angeles
[181] Chen A, Chuyanov V, Zhang H, Garner S M, Lee S S, Steier W H, Chen J, Wang F, Zhu J, He M, Ra Y, Mao S S, Harper A W, Dalton L R and Fetterman H R 1999 *Opt. Eng.* **38** 2000
[182] Chen A, Chuyanov V, Zhang H, Garner S, Lee S S, Steier W H, Chen J, Wang F, Zhu J, He M, Ra Y, Mao S S H, Harper A W, Dalton L R and Fetterman H R 1998 *Proc. SPIE* **3281** 94
[183] Chen A, Chuyanov V, Zhang H, Garner S, Steier W H, Chen J, Zhu J, He M, Mao S S H and Dalton L R 1998 *Opt. Lett.* **23** 478
[184] Grote J S, Zetts J S, Drummond J P, Nelson R L, Hopkins F K, Zhang C H, Dalton L R and Steier W H 2000 *Proc. SPIE* **3950** 108
[185] Grote J G, Drummond J P, Zetts J S, Nelson R L, Hopkins F K, Zhang C, Dalton L R and Steier W H 2000 *Mater. Res. Soc. Symp. Proc.* **597** 109
[186] Grote J S, Zetts J S, Zhang C H, Nelson R L, Dalton L R, Hopkins F K and Steier W H 2000 *Proc. SPIE* **4114** 101
[187] Grote J G, Zetts J S, Nelson R L, Hopkins F K, Dalton L R, Zhang C and Steier W H 2001 *Opt. Eng.* **40** 2464
[188] Grote J G, Zetts J S, Nelson R L, Hopkins F K, Huddleston J B, Yaney P P, Zhang C H, Steier W H, Oh M C, Fetterman H R, Jen A K Y and Dalton L R 2001 *Proc. SPIE* **4470** 10
[189] Diggs D E, Grote J G, Davis A A, Zhang C H, Zetts J S, Nelson R L, Dalton L R, Yaney P P and Hopkins F K 2002 *Proc. SPIE* **4813** 94
[190] Leovich M, Yaney P P, Zhang C H, Steier W H, Oh M O, Fetterman H R, Jen A K Y, Dalton L R, Grote J G, Nelson R L, Zetts J S and Hopkins F K 2002 *Proc. SPIE* **4652** 97
[191] Mao S S H, Ra Y, Guo L, Zhang C, Dalton L R, Chen A, Garner S and Steier W H 1998 *Chem. Mater.* **10** 146
[192] Song S, Lee S J, Cho B R, Shin D H, Park K H, Lee C J and Kim N 1999 *Chem. Mater.* **11** 1406
[193] Brasselet S and Zyss J 1998 *Proc. SPIE* **3469** 154
[194] Ma H, Jen A K Y, Wu J, Wu X, Liu S, Shu C F, Dalton L R, Marder S R and Thayumanavan S 1999 *Chem. Mater.* **11** 2218
[195] Wang C, Zhang C, Wang P, Zhu P, Ye C and Dalton L R 2000 *Polymer* **41** 2583
[196] Zhang C, Wang C, Dalton L R, Zhang H and Steier W H 2001 *Macromolecules* **34** 253
[197] Zhang C, Wang C, Yang J, Dalton L R, Sun G, Zhang H and Steier W H 2001 *Macromolecules* **34** 235
[198] Wang C, Zhang C, Zhou C, Chen M and Dalton L R 2001 *Macromolecules* **34** 2359
[199] Lee J Y and Park E J 2002 *Polym. Int.* **51** 228

[200] Jeng R J, Chan L H, Lee R H, Hsiue G H and Chang H L 2001 *J. Macromol. Sci.* A **38** 1259
[201] Kim T D, Lee K S, Lee S Y, Kim Y J and Song J W 2001 *Mol. Cryst. Liq. Cryst.* A **371** 337
[202] Jin S H, Kim S H and Gal Y S 2001 *J. Polym. Sci* A **39** 4025
[203] Lee J Y and Park E J 2001 *J. Macromol. Sci.* A **38** 973
[204] Samyn C, Ballet W, Verbiest T, Van Beylen and Persoons A 2001 *Polymer* **42** 8511
[205] Leng W N, Zhou Y M, Xu Q H and Lin J Z 2001 *Polymer* **43** 9253
[206] Leng W N, Zhou Y M, Xu Q H and Liu J Z 2001 *Polymer* **42** 7749
[207] Park L S, Kim S J, Choi S Y and Kim G H 2001 *Mol. Cryst. Liq. Cryst.* A **357** 11
[208] Beltrani T, Bosch M, Centore R, Concilio S, Gunter P and Sirigu A 2001 *J. Polym. Sci* A **39** 1162
[209] Zhang C, Zhang H, Oh M C, Dalton L R and Steier W H 2003 *Proc. SPIE* **4991** at press
[210] Ma H, Wu P, Herguth B, Chen B and Jen A K Y 2000 *Chem. Mater.* **12** 1187
[211] Kang S H, Luo J, Ma H, Barto R R, Frank C W, Dalton L R and Jen A K Y 2003 A hyperbranched aromatic fluoropolyester for photonic applications *Macromolecules* at press
[212] Luo J, Haller M, Li H and Jen A K Y 2003 Highly efficient and thermally stable electro-optic polymer from a reversible crosslinking process *J. Am. Chem. Soc.* submitted
[213] Galvan-Gonzalez A, Stegeman G I, Jen A K Y, Wu X, Canva M, Kowalczyk A C, Zjamg X Q, Lackritz H S, Marder S, Thayumanavan S and Levina G 2001 *J. Opt. Soc. Am.* B **18** 1846
[214] Stegeman G I, Van-Gonzales A G, Canva M, Twieg R, Kowalczyk A C, Zhang X Q, Lackritz H S, Marder S, Thayumanavan S, Chan K, Jen A K Y and Wu X 2000 *Mol. Cryst. Liq. Cryst. Sci. Tech.* B **25** 23
[215] Canva M, Galvan-Gonzalez A, Stegeman G I, Twieg R J, Chan P, Kowalczyk T C and Lackritz H 2000 *Proc. SPIE* **4106** 104
[216] Lee M 2003 *PhD Thesis* University of Southern California, Los Angeles
[217] Drenser K A, Larsen R J, Strohkendl F P and Dalton L R 1999 *J. Phys. Chem.* **103** 2290
[218] Teng C C 1993 *Appl. Phys. Lett.* **32** 1051
[219] Chen A, Chuyanov V, Marti-Carrera F I, Garner S, Steier W H, Mao S S H, Ra Y, Dalton L R and Shi Y 1997 *IEEE Photonics Technol. Lett.* **9** 1499
[220] Chen A, Chuyanov V, Marti-Carrera F I, Garner S, Steier W H and Dalton L R 1997 *Proc. SPIE* **3147** 268
[221] Lee S S, Garner S, Chen A, Chuyanov V, Steier W H, Guo L, Dalton L R and Shin S Y 1998 *Appl. Phys. Lett.* **73** 3052
[222] Dalton L R 2002 *Mater. Today* **5** 38